The Role of Intracellular Calcium Signaling in Regulating Transepithelial Ion Transport by the Malpighian Tubules of *Rhodnius prolixus*

A Thesis Submitted to the College of Graduate Studies and Research in Partial Fulfillment of the Requirements for the Degree of Master of Science in the Department of Physiology at the University of Saskatchewan.

By: Noman Hassan

Permission to Use

In presenting this thesis/dissertation in partial fulfillment of the requirements for a Postgraduate degree from the University of Saskatchewan, I agree that the Libraries of this University may make it freely available for inspection. I further agree that permission for copying of this thesis/dissertation in any manner, in whole or in part, for scholarly purposes may be granted by the professor or professors who supervised my thesis/dissertation work or, in their absence, by the Head of the Department or the Dean of the College in which my thesis work was done. It is understood that any copying or publication or use of this thesis/dissertation or parts thereof for financial gain shall not be allowed without my written permission. It is also understood that due recognition shall be given to me and to the University of Saskatchewan in any scholarly use which may be made of any material in my thesis/dissertation.

Requests for permission to copy or to make other uses of materials in this thesis/dissertation in whole or part should be addressed to:

Head of the Department of Physiology
107 Wiggins Road
University of Saskatchewan
Saskatoon, Saskatchewan S7N 5E5 Canada

OR

Dean College of Graduate Studies and Research
University of Saskatchewan
107 Administration Place
Saskatoon, Saskatchewan S7N 5A2 Canada

Abstract

Intracellular ion and volume homeostasis is fundamental to epithelial cells during water and solute transport. When homeostasis is disrupted, it may result in pathological consequences, e.g. cystic fibrosis. We use *Rhodnius prolixus* Malpighian tubules as a model epithelium to study the mechanisms of intracellular homeostasis in epithelial cells. Previously published research indicates that intracellular calcium (Ca^{2+}) signal may be involved in the intracellular homeostasis in some vertebrate epithelia by mediating the crosstalk between ion transporters. In this thesis, (I) we investigate if Ca^{2+} oscillations are part of crosstalk mechanism between apical and basolateral membrane transporters and, (II) use mass spectrometry (MS)-based proteomics to decipher proteins involved in crosstalk mechanism.

Calcium imaging experiments revealed that the amplitude and the frequency of the intracellular Ca^{2+} oscillations displayed by Malpighian tubule cells correlated with the fluid transport rate. As the transport rate decreased with increasing concentration of the transport blocker, bumetanide, the Ca^{2+} oscillations displayed smaller amplitudes and frequency. Similarly, changes in transcellular potassium (K^+) flux, while maintaining constant fluid secretion rate, caused a concentration-dependent decrease in amplitude and frequency of Ca^{2+} oscillations. These results are consistent with the hypothesis that Ca^{2+} oscillations may code information on ion transport flux that could be a part of the crosstalk mechanism.

To further test the role of Ca^{2+} in regulating intracellular ion homeostasis, we measured intracellular potassium using imaging. Our results show that inhibiting intracellular Ca^{2+} oscillations blocked the ability of the tubule cells to maintain a constant intracellular K^+ concentration after the cells were experimentally forced to instantaneously reduce transcellular K^+ flux. This indicates that in the absence of Ca^{2+} oscillations, the cells are unable to maintain

intracellular K^+ homeostasis, suggesting that Ca^{2+} may be involved in regulating the ability of apical and basolateral transporters to crosstalk.

We induced diuresis with serotonin to simulate crosstalk, which is fundamental to diuresis. MS-based proteomics were used to compare serotonin-stimulated samples with control. The results revealed several proteins of interest with a change in the proteome profile, suggesting a potential involvement in crosstalk mechanism. Of these proteins, we validated the roles of WNK and CAMKII, using conventional techniques. Inhibition of WNK significantly reduced fluid transport and reduced amplitude and frequency of Ca^{2+} oscillations in a dose dependent manner. Whereas, inhibition of CAMKII significantly reduced fluid transport but failed to affect the cell's ability to keep an internal ion homeostasis with low K^+ challenge. This suggests that the WNK pathway may be fundamental to the crosstalk mechanism, whereas CAMKII might not be involved.

In conclusion, there exists a crosstalk mechanism between basolateral and apical membranes of *R. prolixus* Malpighian tubule that is mediated through Ca^{2+} oscillations. MS global proteomic profiling has revealed novel machinery that may be involved in ion transport and be potential markers for crosstalk. However, proteins identified must be further investigated for their physiological role in crosstalk.

Acknowledgements

I would like to thank my supervisors Dr. Juan Ianowski and Dr. George Katselis for giving me the opportunity to work under their supervision. My experience during graduate study has been pleasant and phenomenal due to their sound advice, patience, encouragement and guidance every step of the way. Thank you for being my mentors.

Thank you to my advisory committee members, Dr. Veronica Campanucci and Dr. Lane Baker, for their guidance and especially for making me feel at ease.

A huge thank you to my lab mates for their support, laughter, coffee breaks, ideas and help in making this a reality. I am delighted to find lifelong friends in you all.

Thank you to my friends and family and especially, my fiancé for being my motivation and for being patient in my difficult times.

Thank you to the Department of Physiology for accepting me as a graduate student and for letting me sacrifice countless R. prolixus for the purpose of this study.

Finally, I would like to thank God Almighty for giving me the strength to walk this path and for showering His blessings every step of the way.

Table of Contents

List of Figures

List of Tables

List of Abbreviations

ABC: Ammonium bicarbonate

ACN: Acetonitrile

CAMKII: Ca^{2+}/calmodulin dependent kinase II

CF: Cystic fibrosis

CFTR: Cystic fibrosis conductance regulator

Ca^{2+}: Calcium

Cl^-: Chloride ion

DTT: Dithiothreitol

ENaC: Epithelial Na^+ channel

ER: Endoplasmic reticulum

FA: Formic acid

IAA: Iodoacetamide

ISE: Ion selective electrode

K^+: Potassium ion

MAPK: Mitogen activated protein kinase

MS: Mass Spectrometry

Na^+: Sodium ion

NCC69: Na^+ Cl^- cotransporter 69

NFAT: Nuclear factor of activated T-cells

NF-kB: Nuclear factor kappa-light-enhancer of activated B cell

NHE: Na^+/H^+ exchangers

NKCC: Na^+-K^+-Cl^- cotransporter

OSR1: Oxidative stress-responsive 1 kinase

PBFI: K^+ sensor dye

QTOF: Quadrupole time-of-flight

s: seconds

SCX: Strong Cation Exchange

SERCA: Sarco/endoplasmic reticulum Ca^{2+}-ATPase

SPAK: STE20/SPS1-related proline-alanine-rich protein kinase

TFE: Trifluroethanol

WNK: With No Lysine Kinase 1

1. Introduction

1.1 Epithelial tissue

1.1.1 Epithelial Physiology

The animal body consists of four tissue types: nervous tissue, connective tissue, muscle and epithelial tissue (1). Epithelia are the most ancient of all tissue types and it is to the evolution of multicellular organisms what the cell membrane is to the evolution of the cells (2). Epithelia line all internal and external surfaces of the body (3), serving as a barrier to the external environment as well as allowing the existence of specialized environments within the body (3).

Epithelial cells have diverse functions such as protection from injury or sensing of environmental signal. However, the most important and primordial function is, possibly, transepithelial transport of solutes and water that allows animals to exchange with the environment (e.g. nutrient absorption) or to maintain homeostasis (e.g. urine formation by the nephron) (1, 3).

Epithelial cells are polarized, i.e. they have an apical and a basolateral side, separated by tight or septate junctions. The apical and basolateral membranes express different ion transporters that function in coordinated manner to enable transepithelial transport (3). Ion pumps use energy from ATP hydrolysis to establish and maintain ion gradients, which play a crucial role in driving transepithelial transport (1). Transepithelial ion transport could be paracellular or transcellular. In the paracellular pathway, solutes are transported down their electrochemical gradient through the space between two adjacent epithelial cells. In contrast, transcellular pathway involves transport of substances through the cell. This is achieved with the help of pumps and channels present on the apical and basolateral membranes, which enable the tissue to generate electrochemical gradients that force solutes and water to be transported in the desired direction (1). Both

paracellular and transcellular transport are ultimately dependent on energy consumed by the cell, i.e. active transport (1).

Some epithelial cells, such as those from the Malpighian tubules of the blood-sucking insect *Rhodnius prolixus*, may transfer large quantities of solutes across their cells that, in some extreme cases, may exceed the total cytosolic pool of some ions every 3 seconds (3, 4). This high transport rate requires tight homeostasis of cell volume and intracellular ion composition to ensure that sudden changes in transport across the apical or basolateral membrane do not result in dangerous alteration of the intracellular environment. The homeostatic process necessitates communication between apical and basolateral ion transporters to allow them to work in a coordinated manner and ensure that the transport rate across the apical and basolateral membranes are the same, thus avoiding accumulation or depletion of intracellular solutes. This communication, termed as crosstalk, ensures intracellular ion homeostasis during transepithelial transport (5).

1.1.2 Ion transport crosstalk mechanisms

Epithelial cells must have very effective homeostatic mechanisms to ensure that intracellular ion concentration, cell volume and electrochemical gradient remain compatible with cellular function during rapid transport (3, 5). It has been known for a very long time that the activity of the solute transporters is modulated by other components of the transport machinery to maintain homeostasis (3, 5). The different components of the transport machinery seem to display crosstalk mechanisms that help maintain this equilibrium between solute transport across the apical and basolateral membranes. There are a few examples of crosstalk mechanisms that have been described: (I) coordinated activity of apical sodium (Na^+) channels and basolateral K^+ channels in frog skin (5, 6), (II) coupling of apical rheogenic alanine/2 Na^+ uptake and K^+ channel activity in

intestinal mucosa (5, 7), (III) apical chloride ion (Cl^-) channel activation and multiple basolateral Na^+ transport pathways of secretory acinar cells (5, 8). However, we lack comprehensive understanding of the crosstalk machinery.

1.1.3 The machinery of crosstalk

The intracellular machinery that allows for crosstalk among ion transport systems located in the apical and basolateral membranes is not well understood. Several physiological strategies have been reported to be involved in crosstalk in various vertebrate epithelial cells. In salivary glands and frog kidneys, intracellular Cl^- has been proposed to play an important role in crosstalk by regulating the Na^+-K^+-Cl^- cotransporter (NKCC), Na^+/H^+ exchangers (NHE) and cation channel activity through a Ca^{2+} mediated pathway (8, 9). Cook and coworkers proposed an alternative Ca^{2+}-independent mechanism for crosstalk in salivary glands. They proposed the existence of a yet unknown intracellular receptor that senses intracellular Na^+ and Cl^- concentrations, activates a G protein, triggering the ubiquitination and inactivation of the epithelial Na^+ channel (ENaC) and NHE by the ubiquitin-protein ligase Nedd4 (10, 11, 12). Reddy *et al.* proposed that crosstalk between cystic fibrosis conductance regulator (CFTR) and ENaC in sweat ducts is mediated by changes in intracellular K^+ and pH (13, 14). More recently, Feraille *et al.* proposed that in kidney collecting duct cells, the crosstalk between apical ENaC and basolateral NaK-ATPase is mediated by p38 kinase and involves the endocytosis of transporters to modulate transport rate (15).

1.1.4 The importance of crosstalk: Pathophysiological consequences of crosstalk failure

The importance of these crosstalk mechanisms is highlighted by the pathological processes that emerge from disruption in these pathways, such as cystic fibrosis (CF) and Liddle's syndrome. In CF, the CFTR gene is mutated resulting in an abnormal or reduced functional CFTR protein in the apical plasma membrane of epithelial cells in several organs, including the lungs and airway

(16). The CFTR protein is involved in Cl^- secretion and acts as a regulator of ENaC (17). The mutated CFTR leads to a loss of crosstalk with ENaC resulting in hyperactive ENac, thus altering the direction of fluid transport that ultimately leads to the collapse of cilia and disrupted mucociliary clearance (17).

Liddle's syndrome, defined clinically by hypertension, is another rare genetic disorder that results in dysfunctional crosstalk mechanisms. Mutations in ENaC result in a failure to respond to regulatory mechanisms of ubiquitin proteasome system (18, 19). This loss of negative feedback results in increased Na^+ reabsorption by the distal nephron of the kidneys (19). Hence, this increases plasma volume and blood pressure. .

However, in spite of the importance of the crosstalk mechanisms, we have an incomplete and poor understanding of the molecular mechanisms involved in crosstalk. How does the cell determine the rate of ion transport across the basolateral and apical membranes? How is that information coded and transmitted from one end to the other of the cell to match apical and basolateral transport? These, and others, are fundamental questions on epithelial physiology that need to be investigated.

One of the major difficulties in studying crosstalk is that the activation of crosstalk through experimental procedures, such as the use of transport blockers or the reduction of availability of extracellular ions, often results in the shutdown of the transport process as a cellular protective mechanism. Thus, studying crosstalk requires a model epithelium that allows experimental activation of crosstalk without causing protective shutdown of the epithelial transport process. *R. prolixus* Malpighian tubules may be able to provide this model.

1.2 Insects as models

Insects are the most abundant animal group with more than 1 million species, representing 50% of all living organisms (20). Although insects appear to be most abundant in the tropics, they have successfully exploited almost every ecological niche of the global environment (21, 22). The various ecological niches impose high degree of osmotic stress that is detrimental to most organisms on earth. In response to these extreme environments and food resources, insects have evolved sophisticated osmoregulatory organs for survival. For instance, some species of the family Chironomidae, commonly known as lake flies, are able to survive the ruthless winters of Antarctica by dehydrating its tissues during the winter months (23). Some insect species have adapted to dry foods and environment by producing dry feces thanks to a cryptonephridial system, while others have adapted to enormous liquid meals (24, 25). Thus, insects have evolved sophisticated systems to control osmotic and ionic balances that allow most species to regulate their haemolymph composition and volume within a narrow range under extreme environments.

1.2.1 Osmoregulation in insects:

Osmoregulation is performed by the excretory system which in insects consists of the Malpighian tubules and gut (26, 27). An insect's open circulatory system, does not allow for ultrafiltration to produce urine, as seen in vertebrates. Thus, urine production in insects relies on active solute transport by Malpighian tubules and the consequent flow of osmotically-obliged water into the lumen, producing primary urine (28). The rate of transport achieved by some insect Malpighian tubules is amongst the highest of any epithelial tissue described to date. For example, the Malpighian tubule cells in *R. prolixus* transport at rates equivalent to each cell exchanging their whole volume every 10-15 seconds and intracellular Na^+ and Cl^- every 5 seconds (4, 29).

1.3 *Rhodnius prolixus*

R. prolixus is a heametophagous, blood feeding, insect native of central and South America. *R. prolixus* is medically relevant to humans as it is a vector of *Trypanosoma cruzi,* which causes Chagas' disease (30). However, it is not the insect biting the host that causes the spread of the parasite but rather defecation on the host after the blood meal. It is the natural reaction of the human host to scratch the area of the bite, which causes a wound and a route for the parasite to penetrate the skin. According to World Health Organization, about 6-7 million people have been infected with an estimated 50,000 deaths per year, across the globe (31, 32). *R. prolixus* have 5 nymphal stages before reaching adulthood. The complete life cycle requires from 3 months up to 2 years depending on the environmental conditions. Access to hosts, ambient temperature, humidity, and light cycle are key factors in hatching from the egg and molting from one nymph stage to the other. Initiation of molting and reproduction are processes hormonally regulated and the blood meal triggers both events (33, 34).

1.3.1 Blood Meals

Due to infrequent blood meals, *R. prolixus* have evolved to ingest large amounts of blood at a time, approximately 10-12 times their own body weight (30, 35). The enormous blood meals trigger rapid diuresis for two reasons. First, the ingested blood is hypo-osmotic to its hemolymph and a threat to the internal homeostasis (30). Second, the enormous blood meal causes reduced mobility and increases the risk of predation. Thus, during postprandial diuresis the insect is able to excrete 50% of the ingested blood volume within few hours (36).

1.3.2 Diuresis

Two diuretic hormones, serotonin and corticotropin-releasing factor related peptides, initiate diuresis by stimulating ion transport by the crop (the anterior midgut where the blood meal

is stored) and Malpighian tubules (37, 38). The diuretic hormones initiate the transport of the plasma fraction of blood from crop into the hemolymph, where Malpighian tubules are present. Simultaneously, the diuretic hormones activate the distal part of Malpighian tubules to uptake the fluid secreted by the crop and produce urine through active ion transport.

Current understanding of ion transport by *R. prolixus* tubules proposes that an apical vacuolar-type H^+-ATPase initiates transport by generating an H^+ gradient across the apical membrane (Fig. 1). The H^+ gradient drives Na^+ and K^+ transport into the lumen through an apical $H^+/Na^+(K^+)$ exchanger. Chloride anion (Cl^-) crosses the apical membrane through channels down its electrochemical gradient. The entry of ions across the basolateral membrane is mediated by a basolateral NKCC (37). The transport of ions into the lumen of the tubules creates a small but significant osmotic gradient that drives water into the lumen, producing primary urine (28). The primary urine is modified by the proximal segment of the tubule where potassium chloride (KCl) is reabsorbed into the hemolymph producing the final urine. Urine, along with digestive system waste, is excreted through the rectum as feces.

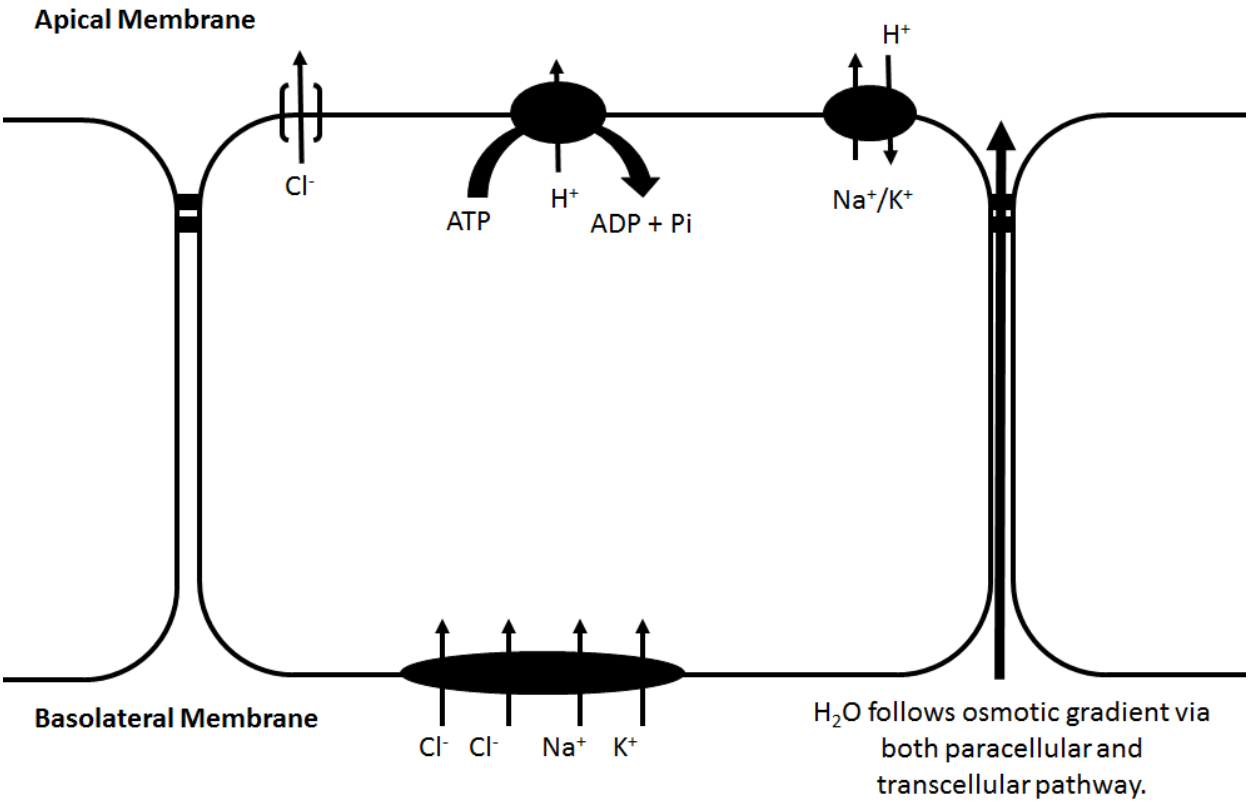

Figure 1: Proposed model of secretion in Malpighian tubules of *R. prolixus* (37). ATPase pumps H^+ ions across the apical membrane. This creates an H^+ gradient which is dissipated in exchange for Na^+/K^+ ions. Cl^- ions passively diffuses through an apical transporter into the lumen. The basolateral NKCC transports Na^+:K^+:2Cl^- into the cell. Water follows the overall gradient towards the lumen.

Epithelial cells in *R. prolixus* Malpighian tubules transport ions at a very high rate and this transport is very tightly regulated to keep the integrity of intracellular functions. In the absence of regulatory mechanisms, cells would deplete intracellular sodium ion (Na^+) and Cl^- content in 5 seconds and the entire haemolymph potassium ion (K^+) content in just 1 minute (37). Thus, Malpighian tubule cells require very efficient transport machinery and effective regulatory mechanisms to prevent catastrophic imbalances in intracellular ion composition. Thus, for our research we use the Malpighian tubules of *R. prolixus* as a model tissue to study crosstalk.

R. prolixus Malpighian tubule cells are an ideal model to study crosstalk because it is possible to experimentally activate crosstalk mechanisms without triggering protective responses or pathology. Our lab has shown that changing extracellular K^+ ion concentration by 80% has no effect on fluid transport rate, which means the tubules are functional. However, within seconds of changing bath K^+ concentrations, the K^+ flux changes by 20% without having any effect on intracellular K^+ concentration (37). This is only possible if there are effective crosstalk mechanisms that allow tubule cells to adjust apical K^+ transport in the face of sudden changes in basolateral intake. Based on this, we hypothesize that an intracellular machinery of crosstalk exists that matches apical and basolateral ion transport to maintain intracellular volume and ion concentration homeostasis.

1.4 Hypothesis

There is a Ca^{2+} mediated intracellular machinery of crosstalk that matches apical and basolateral ion transport to maintain intracellular volume and ion concentration homeostasis in *R. prolixus* Malpighian tubules.

1.4.1 Objectives

1) To test whether intracellular Ca^{2+} signaling is involved in the crosstalk among ion transport proteins in Malpighian tubules of *R. prolixus*.
2) To use mass spectrometry-based proteomics to decipher proteins involved in crosstalk.

2.0 Material and Methods

2.1 Dissection

R. prolixus were obtained from a colony maintained at 25-26 ^{o}C with 60% relative humidity located at the Cardiopulmonary Cluster, College of Medicine, University of Saskatchewan. Malpighian tubules of *R. prolixus* are physiologically identical but differ in size during different nymphal stages. For the ease of experimental setup, 3rd and 5th nymphal stages were used for imaging and secretion assays, respectively. *R. prolixus* were dissected in control saline under a dissecting microscope to isolate Malpighian tubules (Fig. 2A).

The distal (fluid secreting) part of the Malpighian tubule was used, which consists of approximately two-thirds of the tubule length (Fig. 2A). The distal part of Malpighian tubule is composed of single cell lining with uniform secretory properties throughout its length (39, 40).

2.2 Imaging

2.2.1 Calcium Imaging

Third instar *R. prolixus* were dissected at room temperature (20-25 ^{o}C) and bathed in control saline solution. The isolated distal Malpighian tubule was placed in a custom build chamber with a glass bottom treated with poly-lysine. The tubules were submerged in control saline solution containing 5 µmol l^{-1} Fura2-AM dye for 60 minutes (Life Technologies, Burlington, Ontario, Canada) with 1 mmol l^{-1} probenecid (Sigma, St. Lois, MO, USA), and 0.1% pluronic F-127 (Sigma, St. Lois, MO, USA) to facilitate dye loading. Post incubation, the tubules were washed

and submerged in saline solution containing 1 mmol l^{-1} probenecid. The Malpighian tubules were bathed with experimental solutions using a continually running bath system. The preparation was analyzed under a 20X water immersion objective with the fluorescent microscope (BX61W1, Olympus, Tokyo, Japan). Measurements were automatically taken every 0.5 second with each excitation wavelength (340 nm and 380 nm) to create intensity ratios of 340 nm / 380 nm excitation using Metafluor software. As a control for viability of Malpighian tubules, the time spent by tubules outside the insect (post-dissection) was limited to 2-3 hours. Calcium ion oscillations originated in pioneer cells and only those cells were considered for analysis. Amplitude was calculated from the baseline to the peak of each oscillation and frequency was measured from peak to peak. Percentage amplitude/frequency of control was calculated using the following formula:

$$Percentage\ of\ Control = \left(\frac{Treatment}{Control}\right) \times 100$$

2.2.2 Potassium Imaging

Changes in intracellular K^+ were studied using K^+-sensitive fluorescence dye, PBFI. Kasner *et al.* have used PBFI to study changes in intracellular K^+ in response to different transport blockers (41). In this thesis, PBFI is being used to study intracellular K^+ in response to changes in K^+ flux, as an assay to study crosstalk. Tubules were prepared as described above but incubated with 5 μmol l^{-1} K^+ sensor PFBI (Life Technologies, Burlington, Ontario, Canada), as well as 1 mmol l^{-1} probenecid and 0.1% pluronic F-127 for 60 minutes. Post incubation, a tubule was washed and submerged in saline solution containing 1 mmol l^{-1} probenecid. The tubule was stimulated with 1 μmol l^{-1} serotonin before analysis under microscope. The preparation was analyzed under a 40X water immersion objective with the fluorescent microscope. Measurements were automatically taken every 0.5 seconds with each excitation wavelength (340 nm and 380 nm) to create intensity ratios of 340 nm / 380 nm excitation using Metafluor software. A thirty seconds

period was selected for analysis, before and after treatment. The change in ratio for each cell was computed and normalized to control using the formula:

$$Normalized\ value = \left(\frac{(\ Ratio - Control\ Average)}{Control\ Average}\right) * 100\%$$

2.3 Secretion assay

A modified Ramsay assay system was used to measure secretion rate of Malpighian tubules (Fig. 2B, 42). Fifth (5^{th}) instar *R. prolixus* were dissected and full intact Malpighian tubules were isolated and placed in 100 µl droplets of control saline solution under paraffin oil in a sylgard (Sigma, Oakville, ON, Canada) petri dish. The proximal end was pulled out of the control saline droplet and wrapped around a fine steel pin placed in sylgard base (Fig. 2B). The distal part of the tubule in the control saline droplet was stimulated with 1µmol l^{-1} serotonin. The portion of Malpighian tubule coming out of the droplet bath was nicked to allow drainage of secreted fluid. The secreted fluid was collected every 10 minutes for 40-60 minutes using a fine glass probe. The secreted droplets were photographed using a microscope camera (MiniVid, LW Scientific, Lawrenceville, GA, USA). To calculate the secretion rate, the diameter (d) was measured using ImageJ software (NIH, USA) and volume (V) was calculated using the sphere volume (V) equation:

$$V = \frac{4}{3}\pi r^3$$

Subsequently, the volume of droplet was divided by the total time of collection to determine the secretion rate.

2.3.1 K^+ Ion Selective Electrode Measurements

Using previously described procedures, K^+ concentration was measured in secreted droplets using ion-selective electrodes (43). Borosilicate capillaries (World Precision Instruments,

Sarasota, FL, USA) were pulled using a vertical micropipette puller (PE-2, Narishige, Japan). Retention of the hydrophobic ionophore cocktails requires silanization of the interior of ion-selective electrodes. Thus, the electrodes were silanized with dichlorodimethylsilane (Sigma, Oakville, ON, Canada) on a hot plate for 20 minutes at 250 ºC. K^+ selective electrodes were based on potassium ionophore I, cocktail B (Sigma, Oakville, ON, Canada) and backfilled with 1 mol l^{-1} KCl. The reference electrode was filled with 1 mol l^{-1} KCl. The K^+-selective electrode was calibrated in solutions of 15 KCl:135 mmol l^{-1} NaCl and 150 mmol l^{-1} KCl. Only electrodes that displayed a change of ≥50 mV per 10 fold change in ion concentration of the calibration solution were used. To measure K^+ concentration, both ion selective electrode and reference electrode were placed in the fluid droplet. The electrodes were connected to an amplifier (FD223A, World Precision Instrument, Sarasota, FL, USA) and data acquisition system (PowerLab, AD Instruments, Colorado Springs, CO, USA). All measurements were performed in a Faraday cage. Ion concertation in fluid droplet was calculated using the formula:

$$C^d = C^c \times 10^{\Delta V/s}$$

where c^d is the ion concentration, c^c is the ion concentration in one of the calibrating solutions, ΔV is the difference in voltage measured between the secreted droplet and the same calibrating solution, and s is the slope of the electrode measured in response to a 10-fold change in ion activity.

2.4 Drugs

The drugs used in this thesis to test the hypothesis and confirm experimental data include: bumetanide as blocker of NKCC (Tocris, Bioscience, Bristol, UK), BAPTA-AM as intracellular Ca^{2+} chelator (Tocris, Bioscience, Bristol, UK), KN93 as inhibitor of CAMKII (Abcam, Toronto, ON, Canada), ruthenium red as inhibitor of mitochondria Ca^{2+} uniporter (Abcam, Toronto, ON, Canada), Compound B (7-Ethoxy-3-N-(furan-2-ylmethyl)acridine-3,9-diamine) as a WNK signaling inhibitor

(Millipore, Etobicoke, ON, Canada) and thapsigargin as inhibitor of SERCA pump (Sigma, Oakville, ON, Canada).

2.5 Statistics

Results from the physiology experiments in this thesis are presented as mean ± SEM and analyzed using Student's t-test for comparing two groups of data, One-Way ANOVA for 1 variable and more than two groups unless the measurements were repeated over time in which case we used repeated measures Two-Way ANOVA. Post data analyses were performed where applicable. All statistical analyses were done using GraphPad Prism 5 software (GraphPad Software, La Jolla, CA, USA).

2.6 Saline Solutions

A list of all the control saline solution variations used in this thesis is presented in Table 1. The control saline solution, based on known hemolymph composition, contains in mmol l^{-1}: 122.6 NaCl, 14.5 KCl, 8.5 $MgCl_2$, 2.0 $CaCl_2$, 10.2 $NaHCO_3$, 4.3 NaH_2PO_4, 8.6 HEPES and 20 glucose (37). All solutions were adjusted to pH 7.

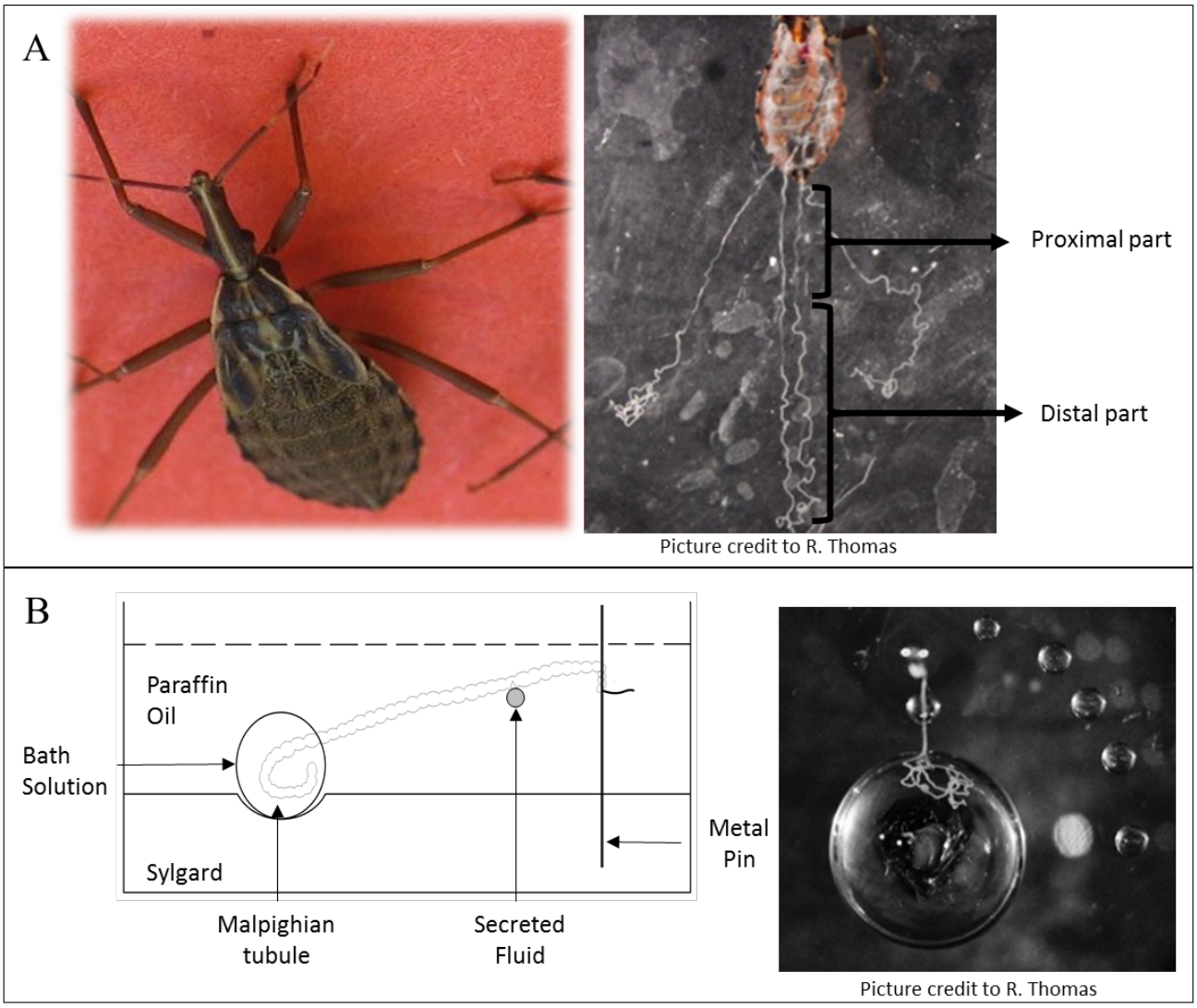

Figure 2: [A] 5th instar *R. prolixus* dissected under a dissecting microscope, depicting Malpighian tubules with proximal and distal parts. [B] Ramsay assay: distal part of the Malpighian tubule is bath in the saline solution with proximal part attached to a metal pin. The distal part is treated in the bath solution and secreted fluid is collected over time.

Table 1: List of Saline solutions and their composition (mmol l^{-1}) used in physiological studies (i.e. calcium imaging)

	Control (14.5 K^+)	**8.0 K^+ Solution**	**6.0 K^+ Solution**	**4.0 K^+ Solution**	**2.0 K^+ Solution**
NaCl	122.6	122.6	122.6	122.6	122.6
KCl	14.5	8	6	4	2
$CaCl_2$	2	2	2	2	2
$MgCl_2$	8.5	8.5	8.5	8.5	8.5
Glucose	20	20	20	20	20
$NaHCO_3$	10.2	10.2	10.2	10.2	10.2
NaH_2PO_4	4.3	4.3	4.3	4.3	4.3
Hepes	8.6	8.6	8.6	8.6	8.6
NMDG*	-	6.7	8.7	10.7	12.7

*NMDG: *N*-methyl-D-glucamine

**All solutions were adjusted to pH 7

2.7 Mass Spectrometry

2.7.1 Dissection

Fifth instar *R. prolixus* were dissected under a dissecting microscope at room temperature (20-30 ^{o}C) and bathed in control saline (Fig 3A). The distal part of the Malpighian tubules was removed and transferred to 1.5 ml tube containing control saline. To isolate enough cytosolic and membrane proteins, we collected 120 tubules in a 1.5 ml tube for each control and serotonin-stimulated group. After isolation, one 1.5 ml tube was stimulated with 1μmol l^{-1} serotonin for 15 minutes; the other was left in Ringer solution with no stimulation. After the 15 minutes period, excess Ringer was removed and tubules were frozen in liquid nitrogen. Tubules were stored at -80 ºC until protein extraction.

2.7.2 Protein Extraction

Membrane and cytosolic proteins were extracted using a modified protocol, first described by Beyenbach and coworkers for *Aedes aegypti* Malpighian tubules (Fig 3B, 44). For this purpose, 100 μl extraction buffer [50 mmol l^{-1} HEPES (pH 7.1), 10 mmol l^{-1} dithiothreitol, 1 mmol l^{-1} PMSF (phenylmethylsulfonyl fluoride) and 5 mmol l^{-1} EDTA (ethylenediaminetetraacetic acid)] was added to the sample tube. In addition, the extraction buffer also contained 1% Halt Protease Inhibitor Cocktail, 2% Phosphatase Inhibitor Cocktail (Waltham, MA, USA), and 0.10% Triton X-100 to avoid protein and potentially modified protein degradation during storage and to facilitate membrane permeabilization. Tubules were homogenized using a plastic mortar and pestle and then lysed by pipetting back and forth the volume in the 1.5 ml tube. Each tube was brought to 1 ml with extraction buffer and sonicated for 30 seconds. Subsequently, tubes were centrifuged at 3000 g at 4 ºC for 10 minutes. Supernatant was collected and centrifuged in 1.5 ml ultracentrifuge tubes at 100,000 g for 60 minutes. The supernatant, which contained cytosolic proteins, was gently

transferred to a new 1.5 ml tubes whereas the pellet formed as a result of the centrifugation, containing membrane proteins, was left intact. Both cytosolic and membrane fractions were stored at -80 ºC until further analysis. Protein concentration was determined by NanoDrop analysis using the BioTek Synergy HT multi-detection plate reader (Winooski, VT, USA). Protein concentrations in the cytosolic fractions were determined to be 6.2 μg μl^{-1} for the control and 5.6 μg μl^{-1} for the serotonin-stimulated groups, respectively. In the membrane fractions, protein concentrations were 1 μg μl^{-1} for the control and 2.2 μg μl^{-1} for the serotonin-stimulated groups, respectively.

2.7.3 Sample preparation

An overview of the sample preparation workflow is illustrated in Figure 4.

2.7.3.1 Protein Digestion

Proteins were digested by in-solution digestion using an in-house developed protocol. Protein fractions, before digestion, were taken out of -80 ^{o}C and thawed on ice. The membrane pellet was re-suspended in a 1% sodium dodecyl sulfate solution while the cytosolic fraction was used as is. Forty five (45) μl of cytosolic (279 μg control, 252 μg serotonin) protein and membrane (45 μg control, 99 μg serotonin) protein fractions were aliquoted for protein digestion. The samples were diluted with 5 μl of 100 mmol l^{-1} ammonium bicarbonate (ABC) buffer (Fisher Scientific, Fair Lawn, NJ, USA) and 50 μl trifluroethanol (TFE, Fisher Scientific, Fair Lawn, NJ, USA) to denature proteins. The samples were treated with 1 μl of 1 mol l^{-1} dithiothreitol (DTT, MP Biomedicals, Solon, OH, USA) while shaking at 300 RPM (Eppendorf Thermomixer, Eppendorf, Mississauga, ON, Canada) at 60 ^{o}C for 60 minutes to reduce disulfide bonds in protein structure. Following that, samples were alkylated with 100 μl of 110 mmol l^{-1} iodoacetamide (IAA, Fisher Scientific, Fair Lawn, NJ, USA) at 37 ^{o}C for 30 minutes on a shaker, covered with aluminum foil, to prevent sulfhydryls back-forming disulfide linkages. The samples were dried in a speedvac

(Labconco, Kansas City, MO, USA). Proteins in the samples were treated with 1 ml cold acetone followed by refrigeration at -80 ^{o}C for 60 minutes to eliminate salts and other interfering compounds (e.g. detergents), which can prevent digestion. The samples were centrifuged at 18000 g for 30 minutes and acetone was carefully removed. This procedure was repeated once more. Samples devoid of interferences were dried in a speedvac and a buffer-containing trypsin (Promega Corporation, Madison, WI, USA) solution (50 ng μl^{-1} trypsin in 1 mmol l^{-1} HCl / 100 mmol l^{-1} ABC) was added to the samples in a 40:1 protein:trypsin. The samples were incubated in a shaker at 300 RPM overnight at 37 ^{o}C. Trypsin buffer at the same ratio was added again in the morning to ensure complete digestion of proteins into peptides. After 2 hours of further incubation at 37 ^{o}C, digested peptides were dried in speedvac and stored at -80 ^{o}C until further analysis.

2.7.3.2 Strong Cation Exchange (SCX)-based Fractionation

Strong cation exchange fractionation was performed using a SCX SpinTips sample preparation kit (Protea Biosciences, Morgantown, WV, USA). SCX SpinTips were used to fractionate complex samples into less complex peptide fractions based on surface charge. The digested protein samples were dissolved in 200 µl of SCX reconstitution solution. Formic acid (FA) was used to adjust the pH to 3. The samples were then loaded on to SCX SpinTip and centrifuged at 2000 g for 6 minutes. This step was repeated 3 times to enhance peptide binding to SCX SpinTip. The flow through at the end of the step was transferred to a 1.5 ml tube for MS analysis. Peptides bound to SCX column were eluted using stepwise concentrations (20, 40, 60, 80, 100, 150, 250, 500 mol l^{-1}) of ammonium formate (Sigma, St. Lois, MO, USA) in 10% acetonitrile (ACN, Fisher Scientific, Mississauga, ON, Canada) at pH 3. 150 µl of ammonium formate (in an increasing concentration) was added to the SpinTip and centrifuged at 2000 g for

6 minutes. The flow through was collected after every centrifugation and transferred to 1.5 ml tube. All flow through solutions were dried in speedvac and stored at -80 ^{o}C.

2.7.3.3 Mass Spectrometry (MS) Workflow

All SCX fractions containing tryptic peptides were reconstituted in 20 µl of MS grade water:ACN:FA (97:3:0.1 v/v) followed by vortexing for 1 to 2 minutes to achieve peptide solubility. The resulting solutions were centrifuged at 18000 g for 10 minutes at 4 ºC. A 15 µl aliquot of each sample was transferred to a mass spectrometry vial (Agilent Technologies Canada Ltd., Mississauga, ON, CA) for liquid chromatography-tandem mass spectrometry (LC-MS/MS) analysis.

All mass spectral analyses were performed on an Agilent 6550 iFunnel quadrupole time-of-flight (QTOF) mass spectrometer equipped with an Agilent 1260 series liquid chromatography instrument and an Agilent Chip Cube LC-MS interface (Agilent Technologies Canada Ltd., Mississauga, ON, CA). Chromatographic peptide separation was accomplished using a high-capacity Agilent HPLC-Chip II: G4240-62021 Phosphochip consisting of a 40 nl titanium dioxide enrichment column (Titansphere, GL Sciences, USA) sandwiched between two high pH stable 100 nl reverse phase enrichment columns (Zobrax Extend 300A, 5µm; Agilent Technologies Canada Ltd., Mississauga, ON, CA) to enrich for phosphopeptides. Samples were loaded onto the enrichment column with a solvent consisting of 95.4% water: 2.0% acetonitrile: 0.6% acetic acid: 2.0% formic acid at a flow rate of 2.0 µl min^{-1}. The phosphochip was operated in dual mode, where the titanium oxide column was first enriched for phosphopeptides and the flow through (non-phosphopeptides) was passed onto the analytical column and separated with linear gradient solvent system. In the second mode, the enriched phosphopeptides were eluted with phospho-elution buffer and separated with a linear gradient solvent system. The linear gradient program was

employed for peptide separation with solvent A (98.9% water: 0.6% acetic acid: 0.5% formic acid) and solvent B (98.9% acetonitrile: 0.6% acetic acid: 0.5% formic acid) on analytical column. The linear gradient was 3–25% solvent B for 50 minutes and then 25–90% solvent B for 10 minutes at a flow rate of 0.3 µl min^{-1}. Positive-ion electrospray mass spectral data were acquired using a capillary voltage set at 1900 V, the ion fragmentor set at 360 V, and the drying gas (nitrogen) set at 225 ºC with a flow rate of 12.0 l min^{-1}. Spectral results were collected over a mass range of 250–1700 (mass/charge; m/z) at a scan rate of 8 spectra s^{-1}. Tandem (MS/MS) data were collected over a range of 100–1700 m/z and a set isolation width of 4 atomic mass units. The top 20 most intense precursor ions for each MS scan were selected for tandem MS with active exclusion for 0.25 min.

2.7.3.4 Protein Identification

Spectral data were converted to a mass/charge data format using Agilent MassHunter Qualitative Analysis Software (Agilent Technologies Canada Ltd., Mississauga, ON, CA) and were processed against the NCBI non-redundant *Drosophila melanogaster* database, using SpectrumMill (Agilent Technologies Canada Ltd., Mississauga, ON, CA) as the database search engine. Search parameters included a fragment mass error of 50 ppm, a parent mass error of 20 ppm, trypsin cleavage specificity and carbamidomethyl as a fixed modification of cysteine. In addition, four stages of database search in variable modification mode were carried out with different sets of variable modifications. In first stage, carbamylated lysine, oxidized methionine, pyroglutamic acid, deamidated asparagine and phosphorylated serine, threonine, and tyrosine were set as variable modifications. In the second stage, validated hits from the first stage were searched using the following variable modifications: acetyl lysine, oxidized methionine, pyroglutamic acid, deamidated asparagine and phosphorylated serine, threonine, and tyrosine. The validated hits from the second stage were searched using semi-trypsin non-specific C-terminus, yielding the third

stage validated hits, which were subsequently searched using semi-trypsin non-specific N-terminus (fourth stage), with no other variable modifications specified. After each stage, SpectrumMill validation was performed at peptide and protein levels [1% False Discovery Rate (FDR)].

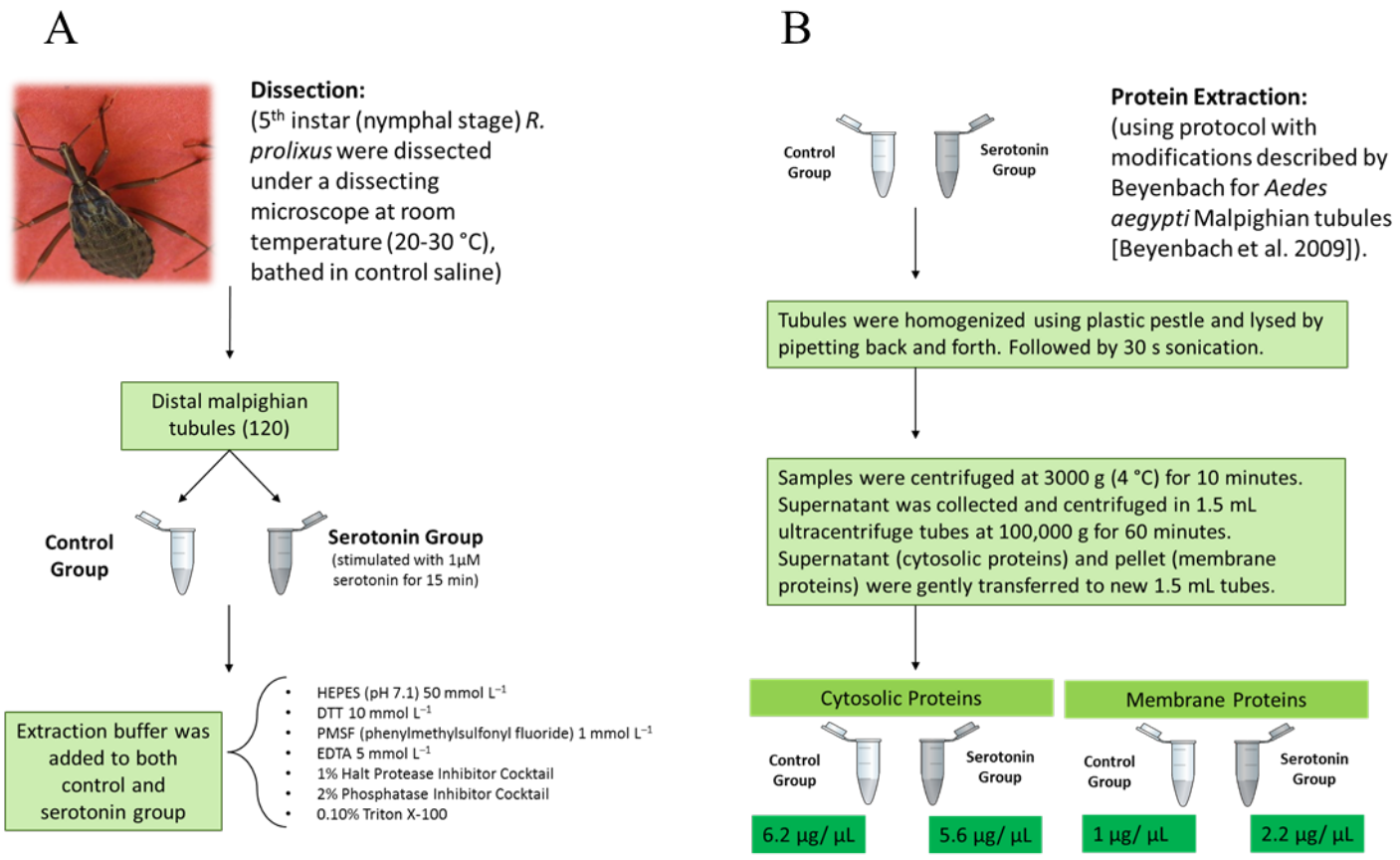

Figure 3: An overview of the extraction method, used to obtain cytosolic proteins and membrane proteins. [A] 120 distal Malpighian tubules were dissected for both control and serotonin-stimulated group. [B] An in house protocol was used to isolate cytosolic and membrane proteins.

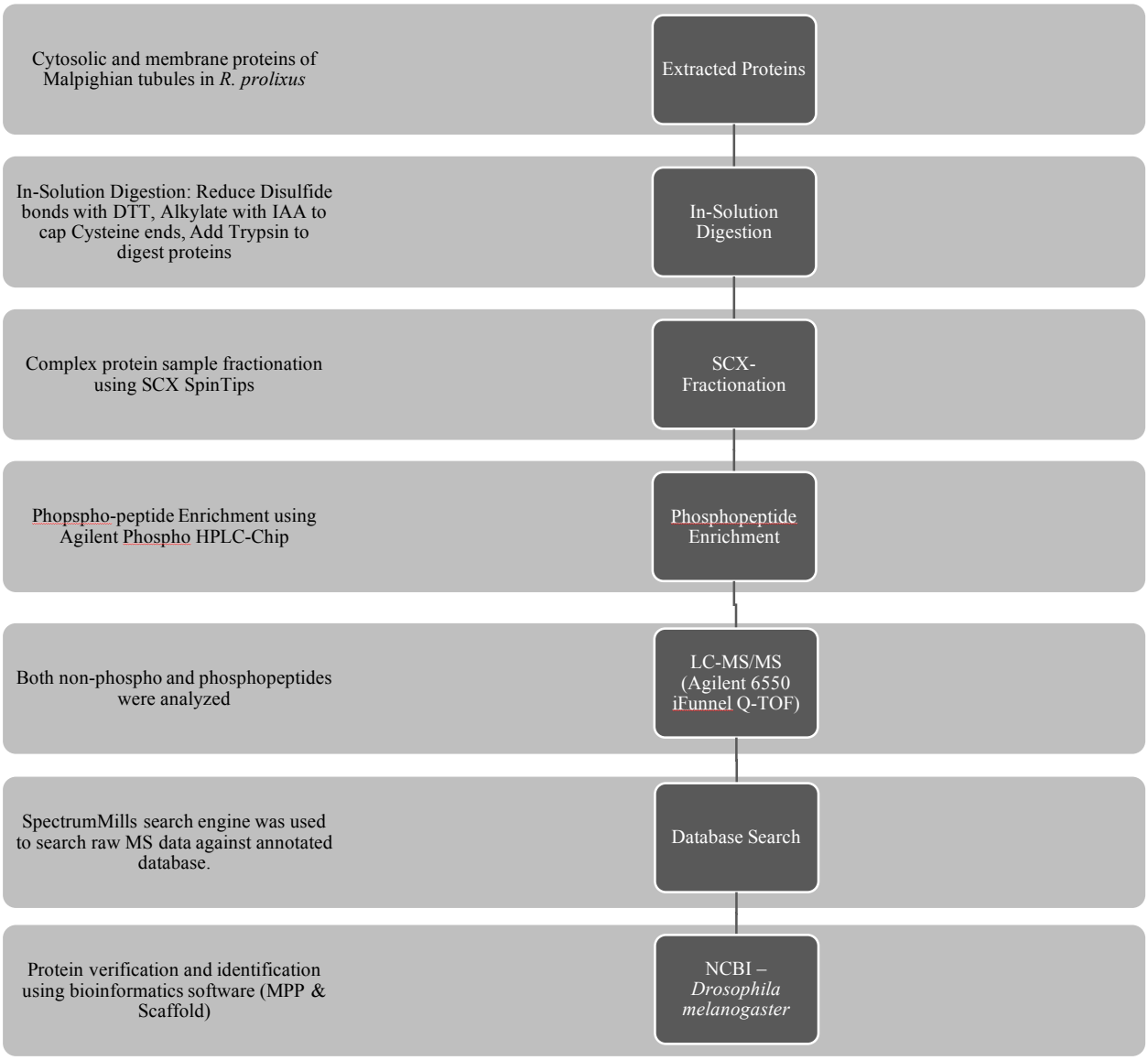

Figure 4: Flow-chart of sample preparation for mass-spectrometry analysis. The extracted proteins were digested, de-salted, and fractionated. The samples were enriched for phosphoproteins using Agilent G4240-62021 Phosphochip and analyzed on Agilent 6550 iFunnel Q-TOF. MS data was run against NCBI-*Drosophila melanogaster* database and analyzed using Bioinformatics software.

3.0 Results

3.1 Ca^{2+} oscillations as a mediator in crosstalk

3.1.1 Effect of changes in liquid secretion rate on Ca^{2+} oscillations

Different concentrations of bumetanide were used to block the bumetanide sensitive NKCC on the basolateral membrane of Malpighian tubule to modulate the fluid transport rate by the cell (37). Ianowski *et al.* showed that the ion transport rate is reduced by bumetanide treatment in a dose dependent manner (37). The effect of different bumetanide concentrations on Ca^{2+} oscillations in epithelial cells of Malpighian tubules is depicted in Figure 5. Intracellular Ca^{2+} oscillations were modulated by alterations in ion flux caused by increasing bumetanide concentrations.

Overall, the amplitude and frequency of the intracellular Ca^{2+} oscillations correlated with the rate of total ion transport across the bumetanide sensitive NKCC. As the rate of ion fluxed decreased (37), with increasing bumetanide concentration, the Ca^{2+} oscillations displayed a smaller amplitude and frequency. As controls, we exposed the Malpighian tubule preparation to the same procedure as experimental preparations but without bumetanide. The control preparations displayed slight difference on intracellular Ca^{2+} signaling amplitude or frequency (see Fig. 6 A and B, 0 μM bumetanide concentration).

The results show a correlation between fluid secretion rate and amplitude and frequency of Ca^{2+} oscillations. The observation is consistent with the hypothesis that intracellular Ca^{2+} signaling may be involved in crosstalk between apical and basolateral transporters. The modulation amplitude and frequency of Ca^{2+} oscillations may code information on the rate of basolateral membrane ion flux.

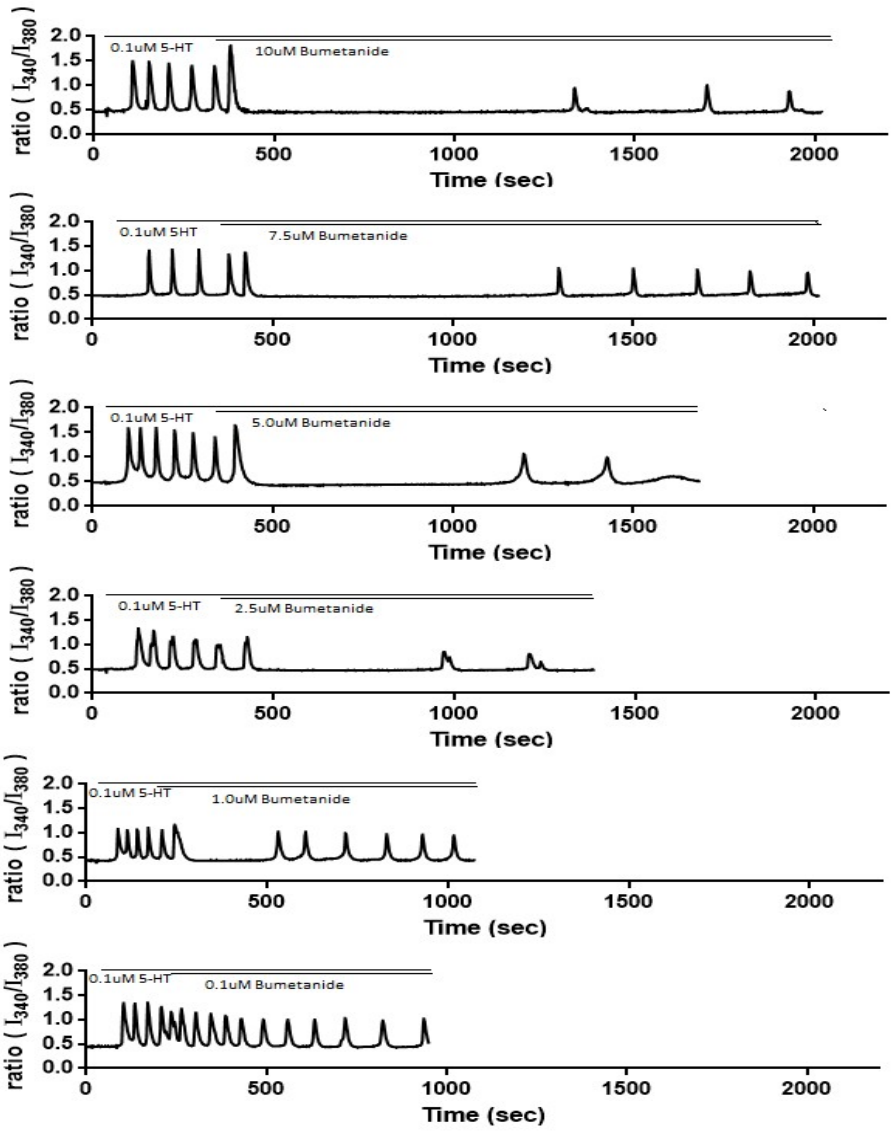

Figure 5: Sample traces of the change in Ca^{2+} oscillations in response to treatment with different concentrations of bumetanide, forcing different rates of ion transport through basolateral NKCC. Tubules were incubated with Fura2-AM, probenecid, and control saline for 60 minutes. After incubation, the Fura2-AM was washed out with saline solution containing probenecid (1 mmol l^{-1}). Serotonin (0.1 µmol l^{-1}) triggered Ca^{2+} oscillations. Different bumetanide concentrations were added, which blocked the basolateral bumetanide sensitive NKCC cotransporter.

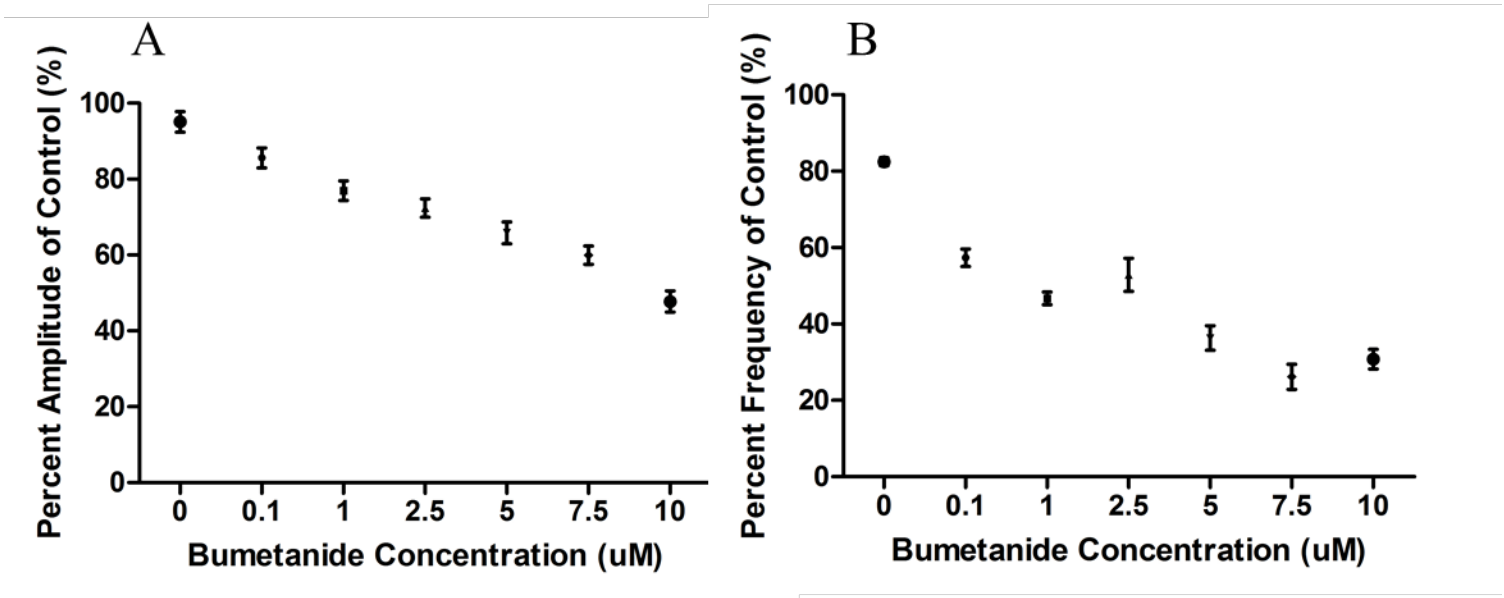

Figure 6: Decrease in [A] amplitude and [B] frequency of Ca^{2+} oscillations in response to different bumetanide concentration (10, 7.5, 5.0, 2.5, 1.0, 0.1 or 0 μmol l^{-1}). The Malpighian tubules were incubated with Fura2-AM, probenecid, and control saline for 60 minutes. After incubation, Fura2-AM was washed out with saline solution (14.5 mmol l^{-1}) containing probenecid (1 mmol l^{-1}). The tubules were stimulated with (0.1 μmol l^{-1}) serotonin. Amplitude and frequency of Ca^{2+} oscillations were calculated before and after adding bumetanide to calculate percentage of amplitude/frequency of control. n = 4-6 tubules per experimental observation.

3.1.2 Effect of changes on K^+ flux rate on intracellular Ca^{2+} signaling

In the previous experiment we tested the effect of reducing fluid secretion rate on intracellular Ca^{2+} signals. Then we decided to test the effect of changes on the flux of a single ion, K^+, while maintaining total fluid secretion rate constant. This can be achieved by exposing the tubules to saline solutions with different concentrations of K^+. Figure 7A shows that there is no difference in fluid secretion rates between different K^+ bath solutions. However, K^+ concentration in the secreted fluid reveals a decrease as bathing saline K^+ concentration is reduced (Fig. 7B). Ianowski *et al.* showed that during this experimental procedure the Malpighian tubules modulate the K^+ flux that may be reduced by ~80 % (from 80 to 20 mmol l^{-1}, Fig. 7B), while maintaining constant intracellular K^+ concentrations (37). This is only possible if the Malpighian tubule cells have a strong homeostatic mechanism, i.e. crosstalk that matches K^+ flux across the basolateral membrane to extrusion across the apical one. This means that as soon as the basolateral membrane K^+ ion concentration is reduced; the cell reduces K^+ extrusion at the apical membrane without a reduction in its total ion transport at the basolateral membrane.

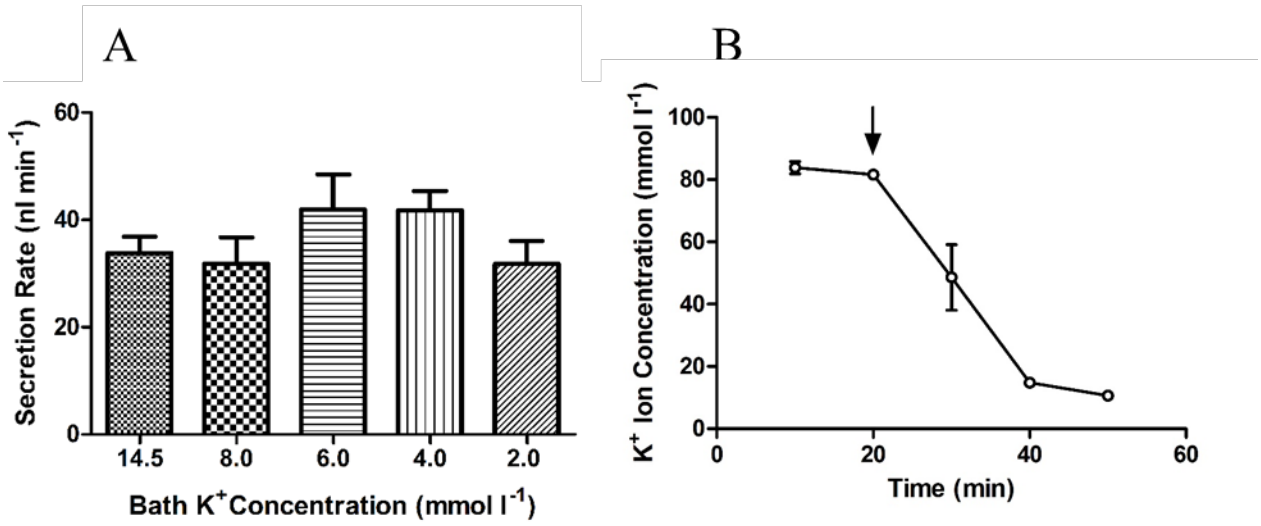

Figure 7: [A] Fluid secretion rate of Malpighian tubules stimulated with 1µmol l^{-1} serotonin; there is no significant difference in transport rate among different K^+ extracellular concentrations (ANOVA, p=0.36, n = 12). [B] K^+ concentration in the secreted fluid. The arrow represents the change in the extracellular bath of K^+ from 14.5 mmol l^{-1} to 2.0 mmol l^{-1}. K^+ concentration at 30 minutes is significantly lower than K^+ concentration at 20 minutes (Student's t-test, p=0.01, n = 6).

The effect of changes on extracellular K^+ ion concentration on intracellular Ca^{2+} oscillations was measured (Fig. 8). The tubules were stimulated with (1μmol l^{-1}) serotonin in control saline solution (14.5 mmol l^{-1} K^+), which initiated intracellular Ca^{2+} oscillations. After the tubule cells displayed 2 to 5 complete Ca^{2+} oscillations, the extracellular K^+ bath was decreased.

The decrease in extracellular K^+ triggered modulation of Ca^{2+} oscillations (Fig. 8). The decrease in extracellular K^+ concentration caused a concentration-dependent decrease in amplitude and frequency of Ca^{2+} oscillations (Fig. 9 A, B). The greater the decrease in K^+ concentration, the greater the impact on Ca^{2+} oscillations. This is consistent with the hypothesis that Ca^{2+} oscillations may be part of a crosstalk mechanism and may carry information on ion flux between the two membranes.

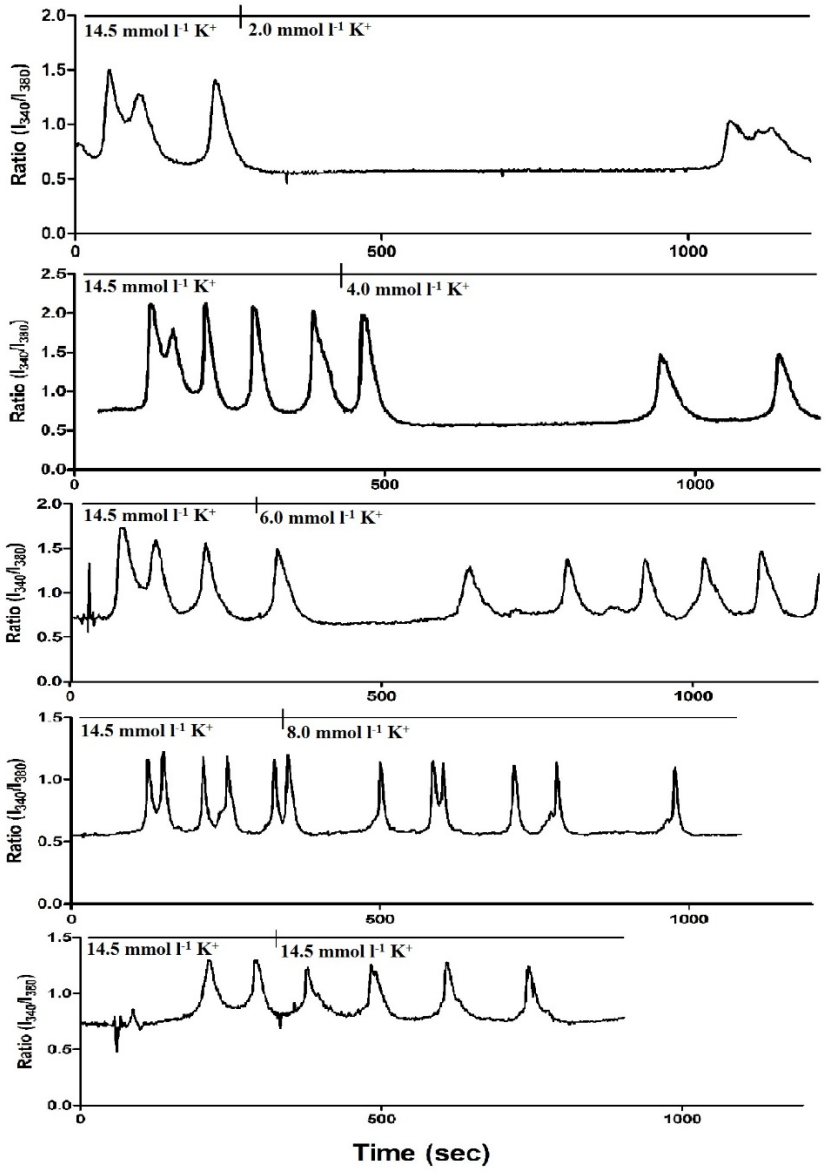

Figure 8: Sample traces of Ca^{2+} oscillations in response to change in extracellular K^{+}. The Malpighian tubules were incubated with Fura2-AM, probenecid, and control saline for 60 minutes. After incubation, Fura2-AM was washed out with saline solution (14.5 mmol l^{-1}) containing probenecid (1 mmol l^{-1}). The tubules were stimulated with (1µmol l^{-1}) serotonin.

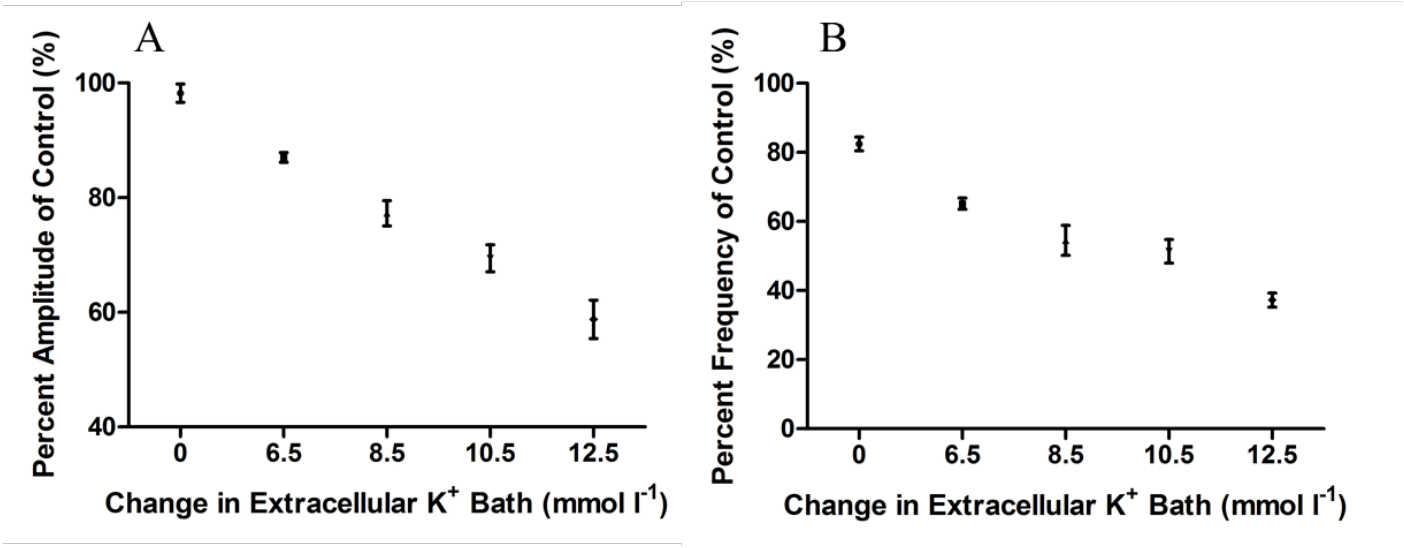

Figure 9: Decrease in [A] amplitude and [B] frequency of Ca^{2+} oscillations mediated by the change in extracellular K^+. The Malpighian tubules were incubated with Fura2-AM, probenecid, and control saline for 60 minutes. After incubation, Fura2-AM was washed out with saline solution (14.5 mmol l^{-1}) containing probenecid (1 mmol l^{-1}). The tubules were stimulated with (1µmol l^{-1}) serotonin. Amplitude and frequency of Ca^{2+} oscillations was calculated before and after extracellular K^+ bath change. n = 4-6 tubules per experimental observation.

3.1.3 Effect of blocking Ca^{2+} oscillations on crosstalk

3.1.3.1 Effect of BAPTA-AM on fluid and K^+ flux

Our results above suggest that intracellular Ca^{2+} oscillations may be part of a crosstalk mechanism that ensures intracellular homeostasis during changes in ion and fluid flux. Thus, we decided to test whether blocking intracellular Ca^{2+} oscillations blocks homeostasis. We decided to test the ability of the cell to maintain intracellular K^+ concentration constant when the cell is challenged with variations in extracellular K^+ concentration. This treatment forces the cell to trigger crosstalk to ensure that K^+ intake through the basolateral membrane is matched by the apical side. If Ca^{2+} plays a significant role in the crosstalk between apical and basolateral membranes, incubation with the Ca^{2+} chelator BAPTA-AM, which blocks Ca^{2+} oscillations (30), should reduce the ability of the cell to perform crosstalk and would result in an inability to respond to K^+ concentration challenge.

Our results show that incubation with BAPTA-AM blocked the ability of the preparations to respond to the K^+ concentration change challenge. Control tubules responded to low K^+ condition by reducing K^+ transport and, thus, reduced K^+ concentration in the secreted fluid (Fig 10 A). At the same time the fluid secretion rate remained constant (Fig 10 B). In contrast, BAPTA-AM treated preparations fail to reduce K^+ flux and the secretion rate was reduced by the low K^+ concentration challenge. This suggests that control preparations were able to conserve intracellular K^+ homeostasis by reducing K^+ secretion at the apical membrane, while BAPTA-AM treated preparations fail to modulate K^+ flux. Thus, we decided to directly measure the effect of BAPTA-AM on intracellular K^+ homeostasis.

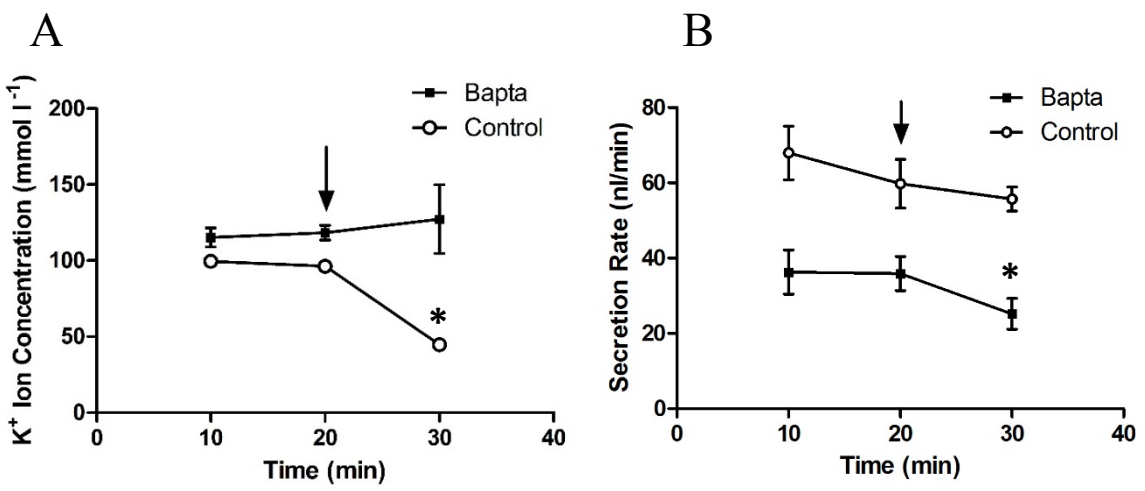

Figure 10: The Malpighian tubules were incubated with BAPTA-AM (300 µmol l^{-1}) prior to stimulation with serotonin (1µmol l^{-1}). The secreted fluid was collected at every 10 minutes interval. At 20 minutes (arrow) the extracellular K^+ bath was changed from 14.5 mmol l^{-1} to 2.0 mmol l^{-1}. The secreted fluid droplets were measured using ISE for K^+ concentration. [A] K^+ measurement in secreted fluid was measured using ISE for K^+ concentration. There is no significant difference K^+ concentration between 20 and 30 minutes in BAPTA treated group (repeated measures two-way ANOVA, p=0.7, n = 10). However, there is a significant difference in K^+ concentration between 20 and 30 minutes in the control group (repeated measures two-way ANOVA, p>0.003, n=5). [B] Secretion rate of secreted fluid was measured. There is no difference in secretion rate between 20 and 30 minutes in the control group (repeated measures two-way ANOVA, p=0.3441, n = 6). However, there is a significant difference between 20 and 30 minutes in the BAPTA treated group (repeated measures two-way ANOVA, p=0.0190, n = 9).

3.1.3.2 Effect of BAPTA-AM on intracellular K^+

We exposed the preparations to the same experimental low K^+ concentration challenge and measured the change on intracellular K^+ using PBFI. PBFI has been used to study intracellular K^+ in mesangial cells of rats (41). In control preparations the tubules suffered a change in intracellular K^+ that was significantly smaller than those suffered by tubules incubated in BAPTA-AM (Fig. 11 A and B). These results indicate that intracellular Ca^{2+} signaling may be involved in K^+ homeostasis and they are consistent with the hypothesis that Ca^{2+} is involved in crosstalk.

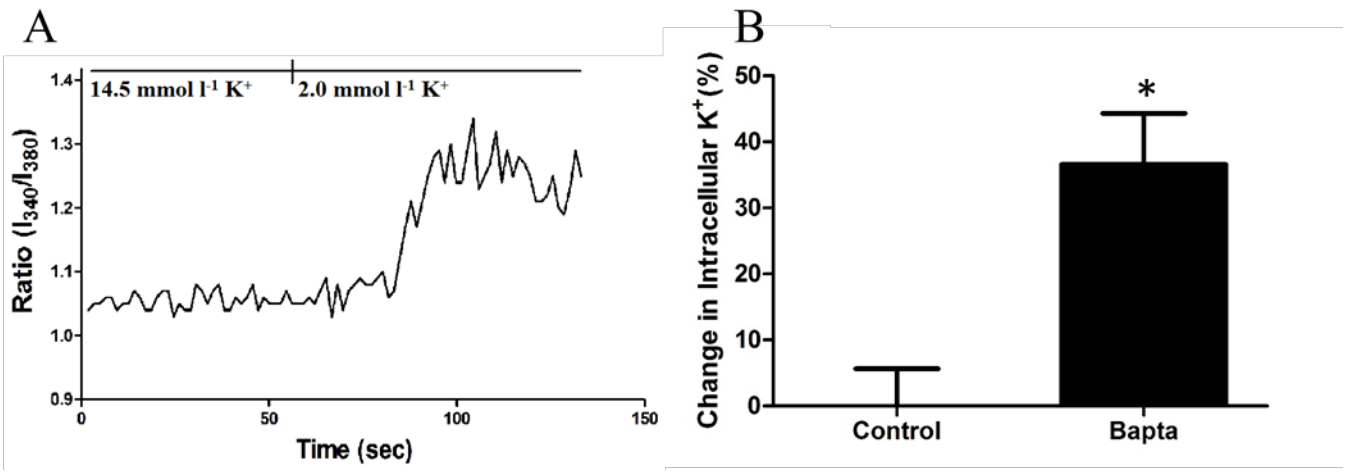

Figure 11: Potassium imaging revealed changes in [A] sample trace of an intracellular K^+ measurement in the BAPTA treated tubule and [B] change in intracellular K^+ fluorescence in control and BAPTA-AM treated tubules. The Malpighian tubules were incubated with PBFI, probenecid in control saline for 60 minutes. After incubation, the PBFI was washed out with saline solution (14.5 mmol l^{-1}) containing probenecid (1 mmol l^{-1}). The tubules were stimulated with (1 μmol l^{-1}) serotonin 5 minutes before the experiment. There is significant change in intracellular K^+ signaling between control tubules and those incubated with BAPTA-AM (Student's t-test, p=0.0001, n = 7).

3.2 Mass Spectrometry

The results from the Physiology experiments support the hypothesis that Malpighian tubule cells display an efficient crosstalk mechanism between the apical and basolateral membranes that enables the cells to maintain intracellular homeostasis during large changes in K^+ flux. Thus, one can assume that there must be an intracellular machinery that is sensing the change in K^+ uptake at the basolateral membrane and transmitting that information to the apical membrane to maintain a stable intracellular K^+ concentration. To fully understand crosstalk in Malpighian tubules of *R. prolixus*, this intracellular machinery must be investigated. We used MS-based proteomics to try and decipher the mechanism of crosstalk.

In order to comprehensively understand this mechanism, Malpighian tubules were dissected and both and membrane proteins were extracted, identified and characterized. Since, crosstalk is fundamental to diuresis process, MS analysis compared control samples and serotonin-stimulated samples for possible markers of crosstalk machinery. Due to the fact that *R. prolixus* genome is not well annotated, the raw MS data was searched against its closest evolutionary species with well annotated genome, i.e. *Drosophila melanogaster*.

3.2.1 Proteome profile

A total of 2264 proteins were identified in *the cytosol* of control and serotonin-stimulated group. Of these proteins, 631 (27.9%) were unique to control group, 847 (37.4%) proteins were unique to serotonin-stimulated group while 786 (34.7%) proteins found to be common to both control and serotonin-stimulated group (Fig. 12A). Furthermore, 1015 (44.8%) out of the 2264 proteins were phosphorylated, with 335 (33.0%) phosphorylated proteins unique to control group,

465 (45.8%) phosphorylated proteins unique to serotonin-stimulated group and a 215 (21.2%) phosphorylated proteins common to control and serotonin-stimulated groups (Fig. 12B).

A total of 1848 proteins were identified in *the cell membrane* of control and serotonin-stimulated group. Of these, 798 (43.2%) proteins were unique to control, 586 (31.7%) proteins unique to serotonin-stimulated group and 464 (25.1%) proteins were common to both groups (Fig. 13A). Out of the 1848 identified proteins, a total of 795 (43.0%) proteins were phosphorylated; 397 (49.9%) phosphorylated proteins were unique to control group, 283 (35.6%) phosphorylated proteins unique to serotonin-stimulated group and 115 (14.5%) phosphorylated proteins common to both groups (Fig. 13B).

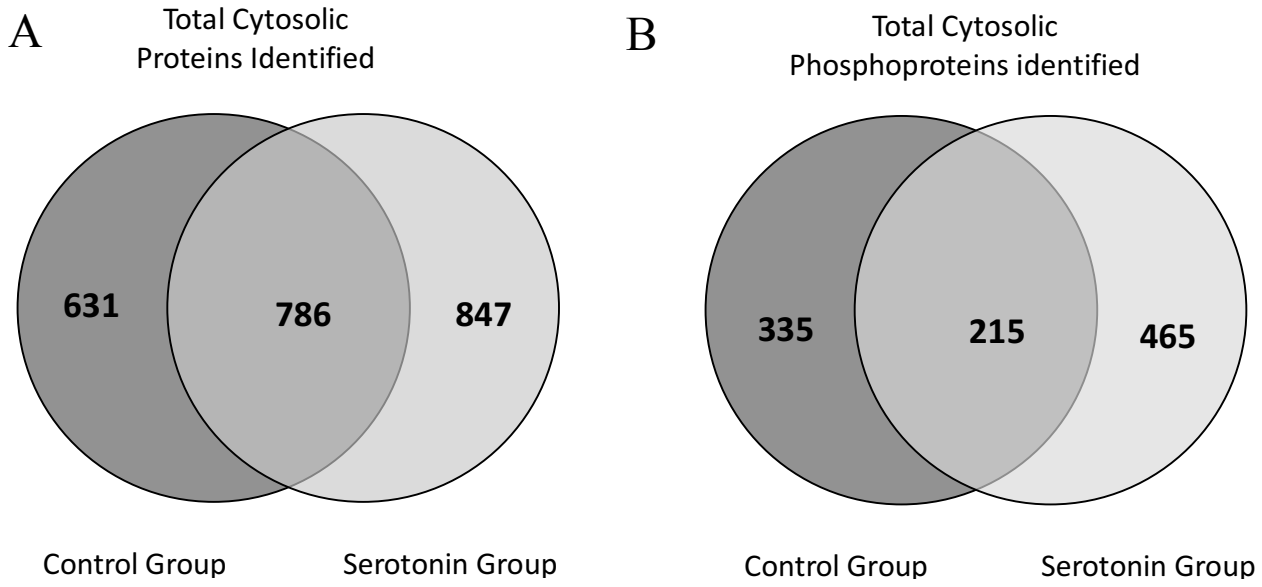

Figure 12: Comparison of number of [A] cytosolic proteins and [B] phosphoproteins identified in control and serotonin-stimulated group. Using SpectrumMill, raw data were analyzed against NCBI *Drosophila melanogaster* database. The results were validated at 1% False Discovery Rate (FDR). The change in proteome (number of proteins and number of post-translational modifications observed) between the control and serotonin-stimulated group highlights the change in intracellular machinery upon serotonin stimulation.

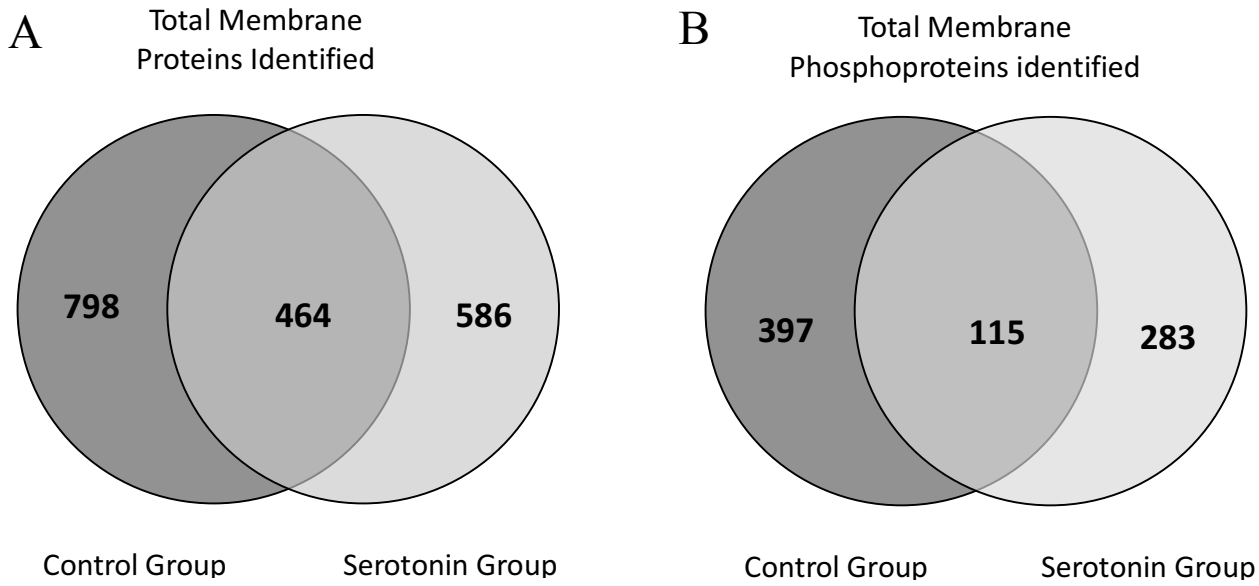

Figure 13: Comparison of number of [A] membrane proteins and [B] phosphoproteins identified in the control and serotonin-stimulated group. Using SpectrumMill, raw data were analyzed against NCBI *Drosophila melanogaster* database. The results were validated at 1% FDR. The change in proteome (number of proteins and number of post-translational modifications observed) between the control and serotonin-stimulated group highlights the change in membrane machinery upon serotonin stimulation.

3.2.2 Validation of MS identified proteins

The MS-based proteomics revealed several proteins of interest with a change in the proteome profile and/or post-translational modifications, suggesting a potential involvement in crosstalk mechanism. Conventional techniques were used to validate the role of MS-based identified proteins.

3.2.2.1 With No Lysine Kinase 1 Pathway

Due to extremely fast and sensitive nature of crosstalk machinery it is unlikely that it may involve *de novo* synthesis of proteins. It is more likely that components of the crosstalk machinery may be modulated through post-translational modifications, such as phosphorylation. Thus we concentrated our attention to kinases, phosphatases and Ca^{2+} binding proteins. We detected a kinase, With No Lysine Kinase 1 (WNK1) that has been shown to phosphorylate and modulate that activity of several ion transporters including NKCC (45, 46).

To test the potential involvement on WNK1 in ion transport and possible role in crosstalk mechanism in *R. prolixus* Malpighian tubules, we tested the effect of a newly developed pharmacological agent, compound B. Compound B is an inhibitor of STE20/SPS1-related proline-alanine-rich protein kinase (SPAK), which is found downstream of WNK1 in its signaling pathway (46, 57). Our results show that compound B inhibits ion transport by *R. prolixus* tubules (Fig.14A) and that this inhibition of ion transport is dose dependent (Fig. 14B). Compound B also reduced both the amplitude and frequency of serotonin-stimulated intracellular Ca^{2+} oscillations in a concentration dependent manner (Fig. 15). These results indicate that WNK1 may be involved in the crosstalk process.

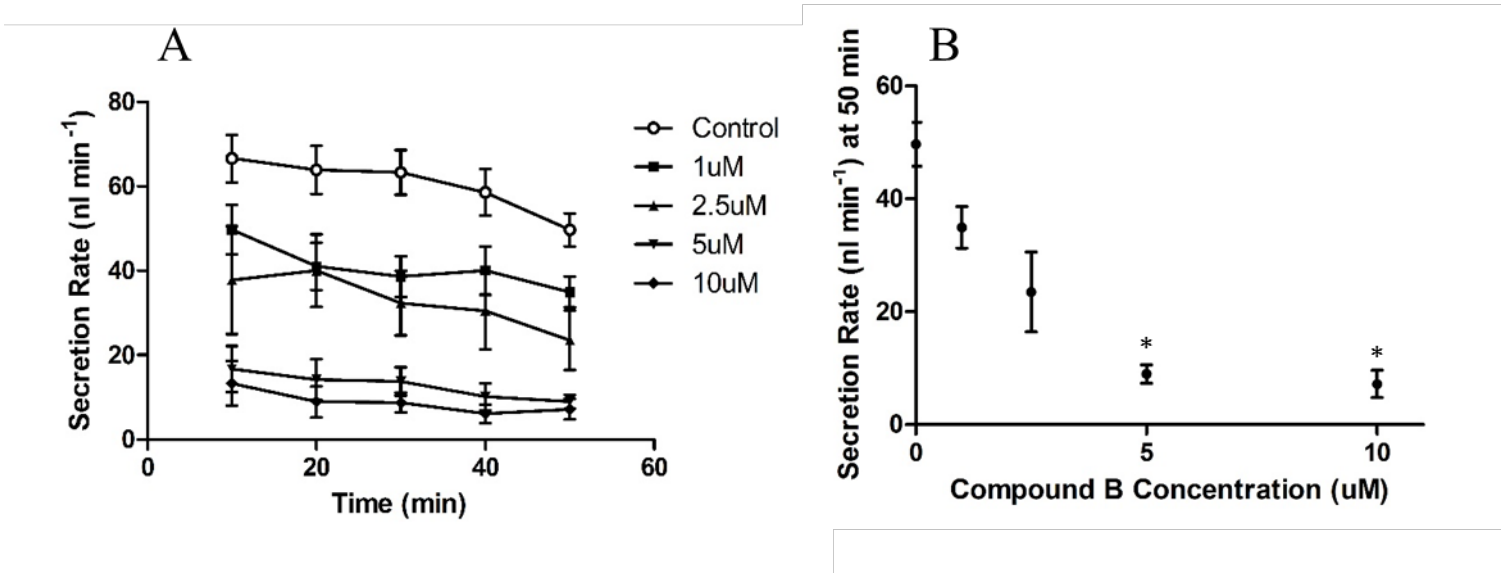

Figure 14: The Malpighian tubules were incubated with different concentration of WNK pathway inhibitor (compound B) in saline solution and stimulated with (1 µmol l^{-1}) serotonin. The secreted fluid was collected every 10 minutes and secretion rate was calculated. [A] Fluid secretion rate of Malpighian tubules with different concentration of compound B, an inhibitor of SPAK, downstream of WNK. In comparison to control, secretion rate was significantly lower with the addition of compound B (repeated measure two-way ANOVA, $p<0.0001$, n = 7, 9, 4, 5, 5 for control, 1, 2.5, 5, 10 µM, respectively). [B] Concentration-response curve showing secretion rate at 50 minutes against different compound B concentrations. In comparison to control (0 µmol l^{-1}), 5 µmol l^{-1} ($p<0.05$) and 10 µmol l^{-1} ($p<0.05$) significantly reduce secretion rate (one-way ANOVA, multiple comparison test, n = 7, 9, 4, 5, 5 for control, 1, 2.5, 5, 10 µM, respectively).

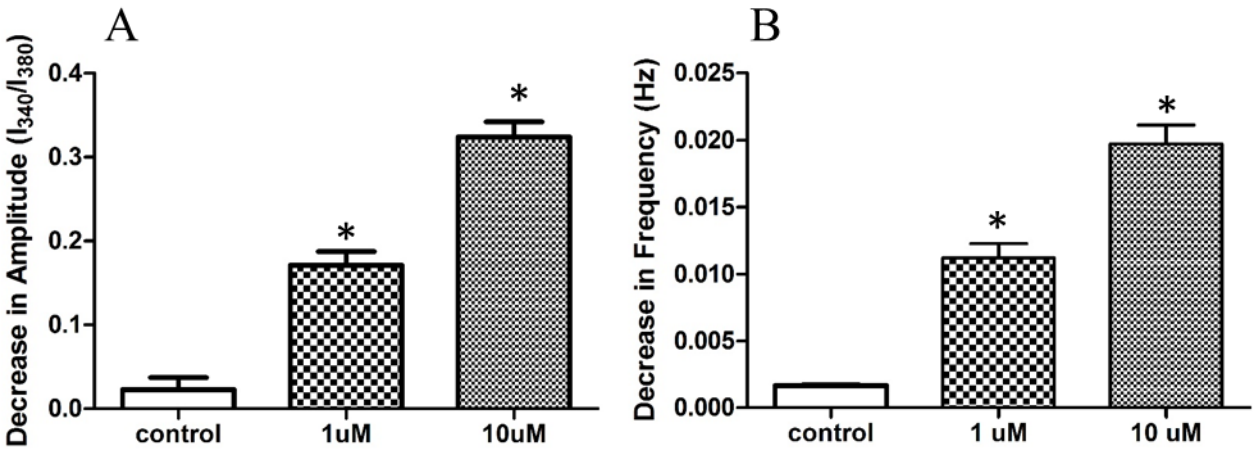

Figure 15: Effect of WNK pathway inhibitor on Ca^{2+} oscillations. The Malpighian tubules were incubated with Fura2-AM, probenecid, and control saline for 60 minutes. After incubation, the Fura2-AM was washed out with control saline (14.5 mmol l^{-1}) containing probenecid (1 mmol l^{-1}). The tubules were stimulated with (1 µmol l^{-1}) serotonin. After 2 to 5 Ca^{2+} oscillations, compound B was added to the saline bath. [A] In comparison to control, amplitude of Ca^{2+} oscillations is significantly reduced with addition of 1µmol l^{-1} (Student's t-test, $p=0.0154$, $n = 27$) and 10 µmol l^{-1} (Student's t-test, $p<0.0001$, $n = 30$) compound B. [B] In comparison to control, frequency of Ca^{2+} oscillations is significantly reduced with addition of 1µmol l^{-1} (Student's t-test, $p=0.0147$, $n = 36$) and 10 µM (Student's t-test, $p<0.0001$, $n = 19$) compound B.

3.2.2.2 Ca^{2+} Binding Protein

Mass spectrometry results also uncovered a "Ca^{2+}/calmodulin dependent kinase II" (CAMKII), found in both control and serotonin groups. Appearance, based on protein signal intensity, of this specific kinase decreased in the serotonin-stimulated group, an observation which may correspond to its interaction with other proteins playing a role in crosstalk. To test the possible contributions of CAMKII to the regulation of tubule function, we tested the effect of the CAMKII inhibitor, KN93 (1 μmol l^{-1}). The results show that inhibition of CAMKII significantly reduced fluid secretion (Fig. 16). To test this further, we decided to measure the effect of CAMKII blockage on intracellular K^+ during low K^+ concentration challenge. As a control, the extracellular K^+ bath was changed from 14.5 mmol l^{-1} to 2.0 mmol l^{-1} prior to incubation of CAMKII inhibitor to test whether the tubules are able to keep an internal K^+ homeostasis. Then, the experiment was repeated in the presence of CAMKII inhibitor. The results indicate that inhibition of CAMKII did not significantly change intracellular K^+ concentration (Fig. 17).

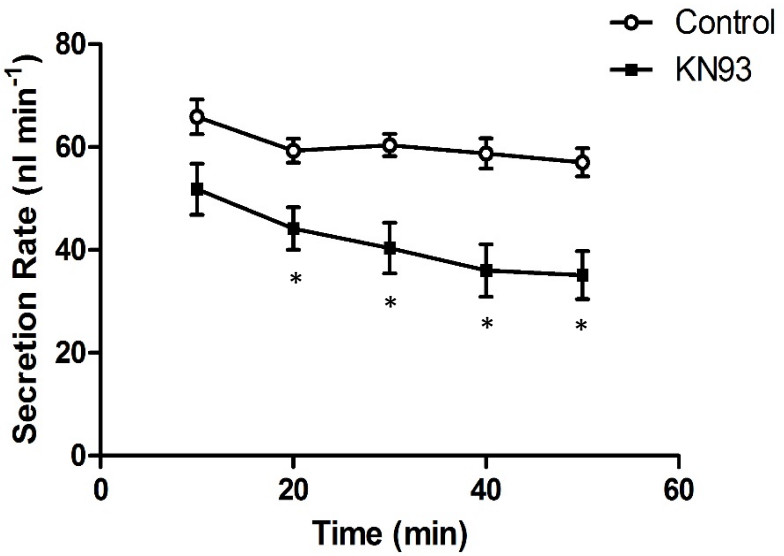

Figure 16: Fluid secretion rate of Malpighian tubules treated with the CAMKII inhibitor, KN93. The Malpighian tubules were incubated with (1 µmol l^{-1}) CAMKII inhibitor in saline solution and stimulated with (1 µmol l^{-1}) serotonin. The secreted fluid was collected every 10 minutes. In comparison to control, incubation of Malpighian tubules with KN93 significantly reduced secretion rate (repeated measures two-way ANOVA, $p<0.0001$, $n = 9$).

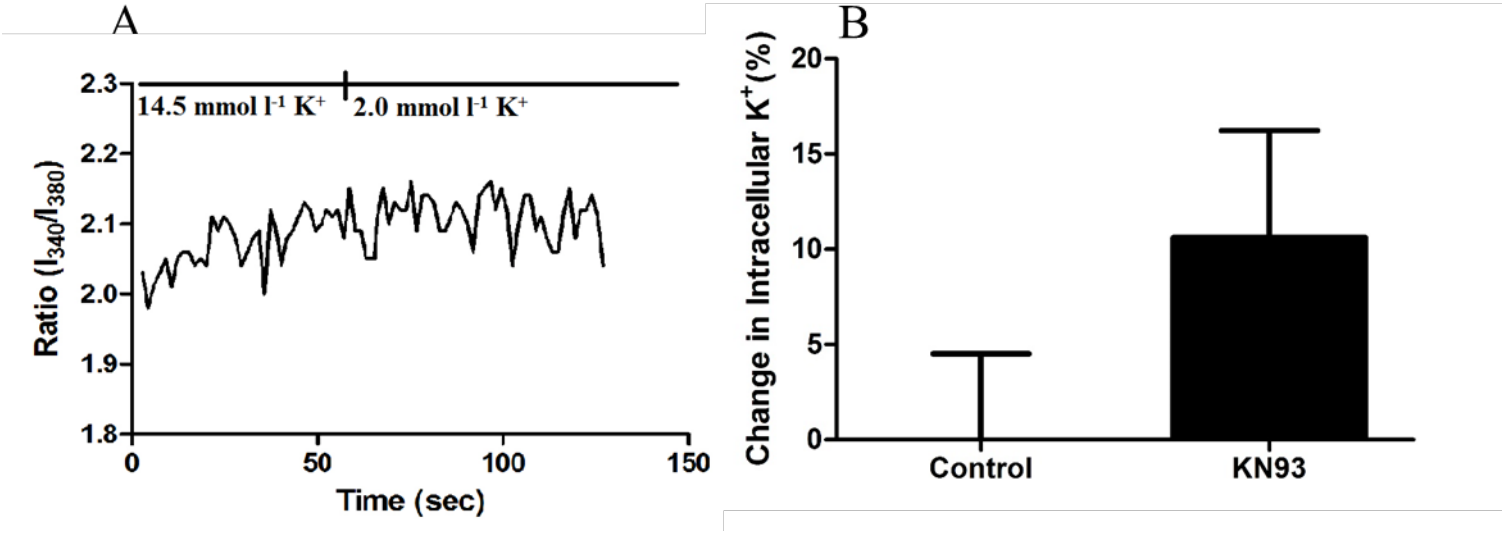

Figure 17: Potassium imaging revealed changes in [A] sample trace of intracellular K^+ fluoresce ratio in KN93 treated tubules and [B] change in intracellular K^+ fluoresce ratio in control and KN93-treated tubules. The Malpighian tubules were incubated with PBFI, probenecid and control saline for 60 minutes. After incubation, the PBFI was washed out with saline solution (14.5 mmol l^{-1}) containing probenecid (1 mmol l^{-1}). The tubules were stimulated with (1µmol l^{-1}) Serotonin and extracellular K^+ bath was changed from 14.5 mmol l^{-1} to 2.0 mmol l^{-1}. There is no significant change in intracellular K^+ concentration in tubules incubated with KN93 (T-test, p=0.14, n = 7).

4.0 Discussion and Conclusion

4.1 Crosstalk mediated through Ca^{2+} oscillations

Crosstalk mechanisms in epithelial cells are fundamental in the coordination of ion transport through channels, pumps, exchangers, and cotransporters. They preserve homeostasis of cell volume and ionic activities while maintaining the physiological function of the tissue during fluctuations in environmental challenges and regulatory signals.

R. prolixus Malpighian tubules display a very efficient crosstalk mechanism (37). Reduction of K^+ concentration in the extracellular bath results in a reduced availability of K^+ at the basolateral membrane. The cell is able to compensate for lack of K^+ by up taking Na^+ instead, without affecting the total cation transport (37). This means, that there is increased number of Na^+ ion going inside the cell and less K^+. If there was no crosstalk between apical and basolateral membrane, this would cause a change in intracellular ion concentration. However, this is not the case, thus transporters on the apical membrane must simultaneously start excreting more Na^+ ions and fewer K^+ ions, preserving intracellular ion homeostasis. This means that the cell is somehow able to detect changes in basolateral ion flux and transmit this information rapidly (i.e. within few seconds, 37) to the transporters at apical membrane. This communication between apical and basolateral membranes, working to preserve intracellular homeostasis, is termed as crosstalk.

Epithelial crosstalk has been described in other systems (8, 9, 10, 13, 15). For instance, epithelial cells in frog kidneys coordinate that total K^+ coming inside the cell with total K^+ going outside, to maintain intracellular K^+ (9). Similarly, rat salivary acinar cells coordinate the total incoming Cl^- with outgoing Cl^- (8), to preserve intracellular ion homeostasis. This is only possible if there exist a system of crosstalk between pumps, channels, and transporters present on apical and basolateral membranes. Thus, in *R. prolixus*, 50% decrease in K^+ flux in response to 90%

decrease in K^+ concentration in the extracellular bath indicates the existence of crosstalk (Fig. 7), as it has been described in other systems.

Our results indicate that intracellular Ca^{2+} signaling seems to play an important role in the crosstalk mechanism in Malpighian tubules of *R. prolixus*. The treatment with bumetanide, a blocker of NKCC that reduces ion transport at basolateral membrane, triggers changes in Ca^{2+} oscillations (Fig. 5). The greater the concentration of bumetanide, the greater the effect on the amplitude of Ca^{2+} oscillations (Fig. 6). These results suggest that there is a correlation between ion transport and Ca^{2+} oscillations and validate the hypothesis that Ca^{2+} oscillations may code information related to ion flux and may be part of crosstalk.

To test the hypothesis further, tubule preparations were bathed in saline solutions with different concentration of K^+ that have no effect on fluid secretion rate but reduce K^+ flux (Fig. 7, 37). Using Fura2-AM, we measured Ca^{2+} oscillations during changes in extracellular K^+ concentration (Fig. 8). We observed that changes in K^+ concentration in the bath modulated the Ca^{2+} oscillations frequency and amplitude (Fig. 9). The degree of changes in amplitude and frequency were dependent on the size of the K^+ changed in the bath, i.e. the greater the change in K^+, the greater the modulation of amplitude and frequency. These results indicate that the Malpighian tubule cells are able to monitor the K^+ flux across the basolateral membrane and communicate this information to the apical membrane. The information could be coded in the change in frequency and amplitude of Ca^{2+} oscillations. Thus, if the Ca^{2+} oscillations were experimentally altered, it would be expected that the ability the cells to maintain intracellular ion homeostasis would fail.

To test this hypothesis, we blocked intracellular Ca^{2+} signaling with the chelator BAPTA-AM. When Ca^{2+} oscillations were blocked with BAPTA-AM (30) the Malpighian tubules cells

did, indeed, lose their ability to conduct crosstalk. Serotonin stimulated tubules bathed in BAPTA-AM lost the ability to respond to changes in extracellular potassium from 14.5 to 2.0 K^+ mmol l^{-1}. Control tubules maintained a constant fluid secretion rate and reduced K^+ flux in response to the change in bath K^+ concentration. In contrast, BAPTA-AM treated tubules did not change K^+ flux and fail to maintain a constant fluid transport rate which decreased by 30% (Fig. 10B). Measurement of intracellular K^+ with PBFI also show that BAPTA-AM treated tubules are unable to maintain intracellular K^+ homeostasis. The results indicate that without BAPTA-AM, i.e. with intact crosstalk mechanism, the tubule cells are able to recognize the decrease in K^+ coming into the cell and trigger a decreased extrusion of K^+ at the apical membrane through a crosstalk mechanism. This is indicative of maintaining intracellular K^+ homeostasis and reducing transepithelial K^+ flux. Intracellular K^+ homeostasis as well as the regulation of transepithelial K^+ flux was blocked by treatment with BAPTA-AM.

Taken together the results indicate intracellular Ca^{2+} oscillations seem to be involved in crosstalk between the basolateral and apical membrane. Without Ca^{2+} oscillations the cells lose their ability to regulate internal ion homeostasis, which is essential to the physiological functions of the cell.

Calcium ion (Ca^{2+}) mediated crosstalk has been reported in other systems. Fowler *et al.* have extensively studied frog kidneys to understand crosstalk mechanism maintaining intracellular K^+ (9). They propose that the crosstalk between cotransporters, pumps, and channels is mediated through increase in intracellular Ca^{2+} concentration (9). Similarly, Robertson *et al.* propose a Ca^{2+} mediated pathway for crosstalk in salivary secretory epithelial cells. They observe a rise in Ca^{2+} concentration that leads to a decrease in intracellular Cl^-, which activates Na^+ transport pathway across basolateral and apical membranes (8). The Ca^{2+} signaling observed in *R. prolixus* tubules

seems to be more complex. Instead of observing a rise in Ca^{2+} concentration, we detect intracellular Ca^{2+} concentration oscillations where amplitude and frequency correlate with ion and fluid transport rate. Calcium oscillations are not common in Malpighian tubules, however there are a number of examples of epithelial tissues that display intracellular waves (47).

Calcium ion (Ca^{2+}) oscillations were first discovered in fish during fertilization (48. 49), and have been documented in both epithelia and non-epithelia cells (50). Calcium ion oscillations are attributed to their diverse role in regulating development and for transferring information from one side of the cell to the other (50, 51). This diverse function of Ca^{2+} oscillations have been attributed to its ability to interact with calcium binding proteins (52) and activate intracellular signaling cascades (48). Furthermore, Ca^{2+} oscillations, reported in hepatocytes of rat, propagate from one cell to the other to coordinate intracellular activities of neighboring cells (49). This is in line with the observation in Malpighian tubule of *R. prolixus* (30), where Ca^{2+} oscillations propagate from one cell to the other. However, the role of propagating Ca^{2+} oscillations is yet to be discovered.

Characterization of Ca^{2+} oscillations revealed that the amplitude and frequency of Ca^{2+} oscillations contain far more information in comparison to static increase in intracellular Ca^{2+} (53, 50, 48, 52). Decoding of Ca^{2+} oscillations requires a decoder (proteins) with multiple Ca^{2+} binding sites that acts as an ON and OFF switch to activate several cellular program, which may include kinases, phosphatases, protein kinase C, calmodulin, and CAMKII (54). Several proteins are proposed in literature as frequency decoder, such as NFAT, NF-κB, CAMKII, MAPK, and calpain (54). Based on our results, we propose that the amplitude and frequency of intracellular Ca^{2+} oscillations code information about ion flux, which is fundamental in keeping internal ion homeostasis.

So far what we have established is the importance of Ca^{2+} in crosstalk mechanism and the manipulation of amplitude and frequency of Ca^{2+} oscillations in response to changes in ion flux. Nevertheless, many questions remind unanswered: how does the cell monitor which ions are coming inside the cell? At what flux rate? How is this information coded and mediated through Ca^{2+} oscillations? These are all questions that need to be investigated in order to fully understand crosstalk mechanism.

Crosstalk strategies defined in other systems are able to provide insight on mechanism that may be involved in crosstalk, which could be further investigated. Cook *et al.* propose the existence of an intracellular receptor that is able to monitor intracellular Na^+ concentration independent of intracellular Ca^{2+} (10). Upon changes in intracellular Na^+, the receptor is able to activate G protein cascade, thereby manipulating the activity of Na^+ channels (10). Ferraille *et al.* propose the involvement of p38 kinase signaling in regulating the endocytosis of Na^+, K^+-ATPase in order to preserve intracellular Na^+ homeostasis (15). Whereas, Wu *et al.* propose the involvement of WNK-SPAK/OSR1 kinase cascade in regulating intracellular ion homeostasis in response to hypotonicity in *D. melanogaster* renal tubule (55).

Thus, to fully understand the crosstalk mechanism in Malpighian tubules of *R. prolixus* and to decipher proteins that may be involved we employed mass spectrometry-based proteomics analysis to generate hypothesis, which could be tested using conventional physiological techniques.

4.2 Mass Spectrometry as 'hypothesis generator'

Poor understanding of the proteins involved in crosstalk mechanism along with lack of pharmacological agents available, led us to pursue MS-based proteomics study to identify potential components of the intracellular machinery of crosstalk. In line with the notion that this proteomic

study is a 'hypothesis generator', the cytosolic and membrane proteins of control and serotonin-stimulated groups were analyzed to identify intracellular proteins and their interactions with apical and basolateral membrane. The change in proteome between control and serotonin-stimulated groups would highlight proteins involved in diuresis (ion transport) process. Consequently, proteins of interest could be further tested in physiological studies, which would unveil proteins of interest in crosstalk.

Raw MS data were initially run against *R. prolixus* database, the majority of proteins identified had unknown biological functions because the *R. prolixus* database is poorly annotated. Thus, it was decided to run the raw MS data against the closest evolutionary species with a well-annotated database, i.e. *D. melanogaster.*

Comparison between control and serotonin-stimulated group showed changes in proteome profile (Fig. 12, 13). This indicates that upon serotonin stimulation, cytosolic and membrane protein profiles change. This could be the result of protein-protein interaction, protein degradation or post translational modifications of proteins. Due to the fast nature of the crosstalk mechanism, it was hypothesized that post translational modifications will be fundamental to deciphering crosstalk mechanism. Thus, we concentrated on kinases, phosphatases and Ca^{2+} binding proteins, which are prone to post translational modifications and due to their possible role in crosstalk mechanism (10, 11, 15).

A comprehensive list of proteins of interest identified and characterized in the cytosol and membrane fractions isolated from the Malpighian tubules in *R. prolixus* is found in Appendix I, Tables 2 and 3, respectively.

4.2.1 Proteins involved in ion transport

Results confirmed the presence of several proteins that might be playing a role in ion transport in *R. prolixus*. V-ATPase subunit A & B, calreticulin, and cAMP dependent protein kinase have been proposed to be involved in the regulation of ion transport in the mosquito species, *Aedes aegypti* (44). Not only were these proteins common among the control and serotonin-stimulated group but their MS signal intensity, a relative qualitative indicator of the level of protein presence, changed upon stimulation with serotonin.

V-type ATPase subunit A and B

V-type ATPase is responsible for creating an H^+ ion gradient across the apical side of Malpighian tubule cells, initiating transepithelial transport in diuresis (44). In comparison to control, the presence of V-type ATPase unit A and B seems to decrease in serotonin-stimulated group in the cytosol. This may indicate that these subunits are recruited to the apical membrane, increasing transepithelial transport. This is consistent with an increased presence of V-type ATPase unit A and B in serotonin stimulated membrane fraction. These findings are consistent with the proposed movement of V-type ATPase unit A and B from the cytosol to the membrane upon activation of diuresis in *Aedes* Malpighian tubules (43).

Calreticulin

Calreticulin is a Ca^{2+} binding protein (56). In the cytosol, its presence drops in the serotonin-stimulated group. While in the membrane fractions, the presence of calreticulin increases in the serotonin-stimulated group. This may indicate that upon serotonin stimulation, calreticulin is removed from the cytosol, possibly interacting with a membrane protein(s). These findings are in line with the findings of Beyenbach *et al.*, where they observed removal of calreticulin from the cytosol upon diuresis activation (43).

cAMP dependent protein kinase 1, isoform D

cAMP dependent protein kinase 1 is present in the cytosol in both control and serotonin-stimulated group. Its presence seems to decrease in the serotonin-stimulated group, however the phosphorylated form of cAMP dependent kinase seems to increase in serotonin-stimulated group. This observation is indicative that serotonin stimulation causes activation of cAMP dependent kinase, which may phosphorylate other substrates inside the cell. Similar findings have been observed in *Aedes* Malpighian tubules (43).

4.2.2 Possible proteins involved in crosstalk

Crosstalk machinery may include intracellular ion concentration sensors (10), G proteins (12), kinases (15), phosphatases and possibly other components (11).

WNK pathway

Recent work by Alexander *et al.* suggests WNK1 and oxidative stress-responsive 1 kinase (OSR1) may be a part of epithelial cells crosstalk mechanism (45). Both of these proteins are thought to be involved in the regulation of NKCC1 at basolateral membrane and NHE transporter at the apical membrane (46, 57, 58) in vertebrate as well as *D. melanogaster* epithelial cells (59). Interestingly, the WNK pathway activity is modulated by intracellular Cl^- (45) and Ca^{2+} concentrations (60).

Our mass spectrometry data confirms the finding of "WNK homolog isoform E" corresponding to *D. melanogaster* in the cytosolic fraction in the control group but not in the serotonin-stimulated group. This could be that serotonin activates crosstalk mechanism, where WNK is activated and phosphorylates downstream substrates. However, due to protein-protein

interactions that may occur during activation of the mechanism, there is no presence of WNK in the serotonin-stimulated group.

A downstream substrate of WNK pathway, 'Frayed, Isoform A', was found in the cytosol in the serotonin-stimulated group. Frayed is homologous to OSR1, which is found downstream of WNK in vertebrate cells (61). The presence of Frayed in the serotonin-stimulated group indicates the activation of WNK pathway and its downstream effectors.

To confirm the involvement of WNK pathway in the regulation of Malpighian tubule secretion we tested the effect of a newly developed inhibitor, compound B, which binds to SPAK and blocks the binding of WNK to SPAK, thereby blocking WNK signaling pathway (Fig. 14). It is also possible that compound B may also block interaction of SPAK with other proteins (41). Compound B displayed a concentration dependent inhibition of fluid secretion by Malpighian tubules, indicating that the WNK pathway is involved in modulating the ion transport properties of the *R. prolixus* tubules. Blockade of WNK pathway significantly reduced amplitude and frequency of Ca^{2+} oscillations in a dose dependent manner, indicating its possible involvement in crosstalk mechanism. Remarkably, WNK has also been shown to change activity in response to alterations of intracellular Cl^- concentration as well as to respond to changes in intracellular Ca^{2+} via interactions with Ca^{2+} binding proteins (45, 46, 60, 62). Thus, WNK could play a role as a sensor inside the cell, monitoring ion concentration and relaying information to the apical membrane, in order to maintain an internal ion homeostasis.

The membrane fraction revealed the presence of 'Na^+ Cl^- cotransporter 69' (NCC69) in both control and serotonin-stimulated group. NCC69 is a cotransporter homologous to vertebrate NKCC in insects. *R. prolixus* NCC69 is found to be phosphorylated in control group and de-

phosphorylated in serotonin-stimulated group. De-phosphorylation of NCC69 upon serotonin stimulation could be due to crosstalk mechanism and involvement of WNK pathway (40).

Ca^{2+} binding protein

Mass spectrometry results have also unveiled another kinase, "Ca^{2+}/calmodulin dependent kinase II" that might be playing a role in crosstalk mechanism and is found both in control and serotonin-stimulated groups of cytosol fraction. The relative MS signal intensity of this specific kinase tends to decrease in serotonin-stimulated group, which may correspond to its interaction with other proteins playing a role in crosstalk. The role of this kinase was assessed in secretion assays using a commercially available inhibitor KN93 (Fig. 16). Secretion assay showed reduced secretion rate in tubules incubated with KN93. However, inhibition of Ca^{2+}/calmodulin dependent kinase II did not affect the cells' ability to maintain internal K^+ homeostasis, upon change in extracellular K^+ bath (Fig. 17). This indicates that Ca^{2+}/calmodulin dependent kinase II is not fundamental to crosstalk mechanism, but is involved in ion transport.

MS-based proteomics have revealed an array of proteins which may be involved in ion transport and crosstalk mechanism. However, changes in the proteome along with post translational modifications must be further investigated to discover the novelty of these proteins that may be involved in crosstalk mechanism. Once identified and characterized, conventional techniques could be utilized along with pharmacological agents to confirm their role.

4.3 Future Direction

The results in this thesis present novel insights into crosstalk mechanism in epithelial cells of Malpighian tubules in *R. prolixus*. Results point to a crosstalk mechanism between the

basolateral and apical membranes of *R. prolixus* Malpighian tubules that it is mediated through the modulation of the amplitude and frequency of Ca^{2+} oscillations.

Future studies are necessary to focus in investigating the source of Ca^{2+} and the regulation of its release from intracellular stores. Preliminary work has indicated that extracellular Ca^{2+} does not seem to contribute to intracellular Ca^{2+} oscillations. Thapsigargin was used to investigate the role of endoplasmic reticulum in Ca^{2+} oscillations (Appendix I). The results showed, a sudden release of Ca^{2+} upon the addition of thapsigargin, but the cell is able to recover from the excessive release of Ca^{2+} as Ca^{2+} oscillations continue. This indicated that there is another source that is driving Ca^{2+} oscillation. Ruthenium red, a mitochondrial Ca^{2+} uniporter inhibitor (Appendix I), blocked Ca^{2+} oscillations. This preliminary suggests that Ca^{2+} release from the mitochondria may be involved in Ca^{2+} oscillations. Release of Ca^{2+} from mitochondria may be dependent on its membrane potentials (63). Thus, when the extracellular K^{+} concentration is changed, causing a decrease in K^{+} transport inside the cell, this may manipulate the membrane potential of mitochondria and modulate Ca^{2+} release. However, these findings are preliminary and must be further investigated.

Mass spectrometry results must also be further investigated to discover novel proteins of interest and generate new hypothesis, which could be tested using other experimental techniques. For instance, bioinformatics can reveal data and associate them to biological pathways, which in turn may indicate presence of novel proteins and biological pathways. Identifying a sequence of a particular protein of interest could be used to create primers for the purpose of PCR or raise antibodies to perform western blotting and in the process confirm the presence of that protein. Also, RNA silencing could be used to target specific protein of interest to investigate their role in crosstalk.

4.4 Proposed Crosstalk mechanism

Based on our results we propose as a working hypothesis for crosstalk mechanism the model depicted in Figure 18. Changes in incoming ions are detected by an internal sensor system, which may consist of WNK, the mitochondria, and/or another internal sensor. The sensor system triggers Ca^{2+} oscillations that encode the size of the ion flux change in the amplitude and frequency modulation. The Ca^{2+} oscillations activate other substrates, which would include Ca^{2+} binding proteins and, possibly, WNK that modulate the activity of apical transporters to match the new ion flux across the basolateral membrane. The crosstalk mechanism communicates between the apical and basolateral membranes to preserve internal homeostatic conditions.

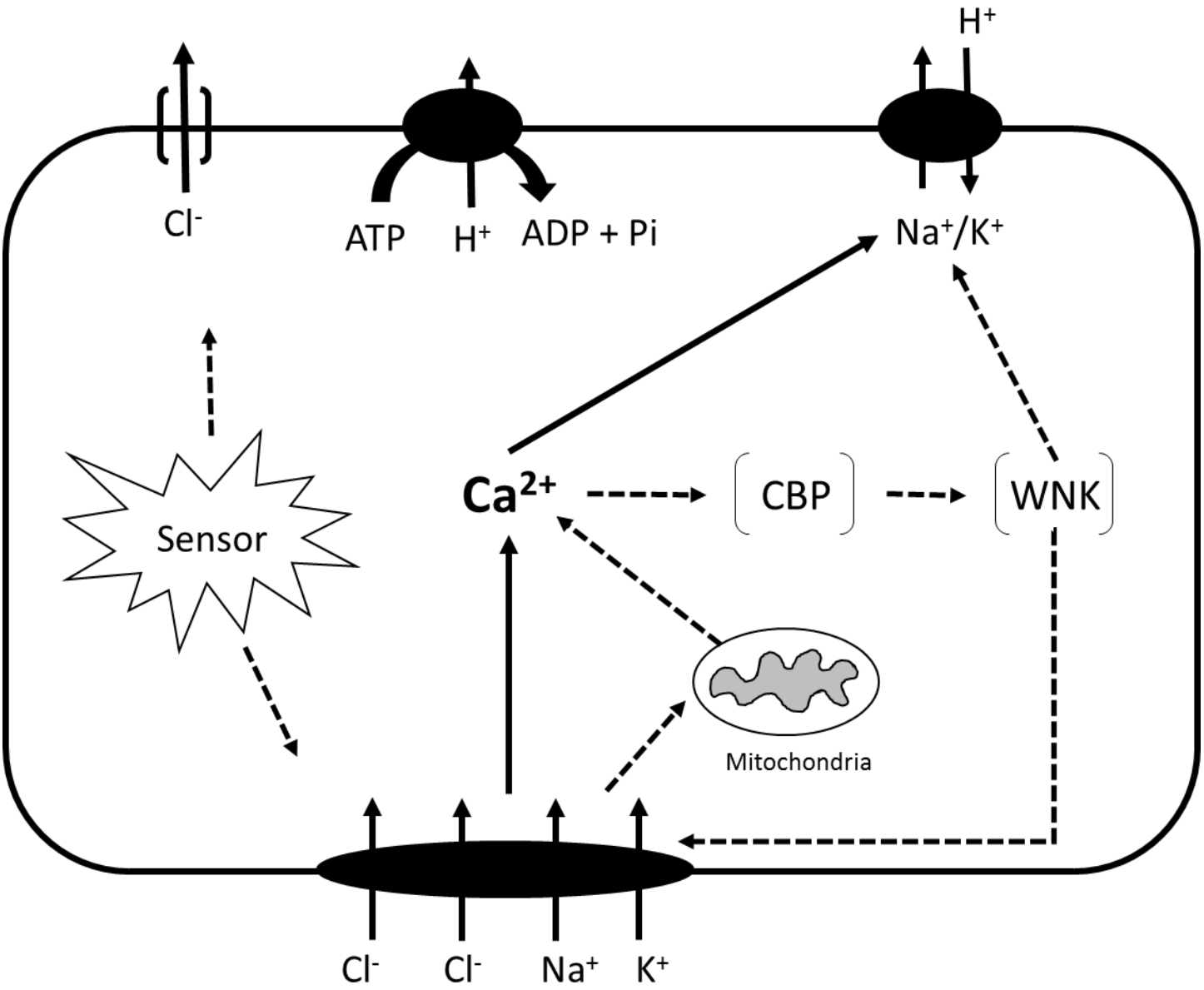

Figure 18: Proposed crosstalk mechanism. Solid arrows represent the establishment of crosstalk mechanism through Ca^{2+} oscillations. Dotted arrows represent probable role of substrate involved in crosstalk mechanism.

5.0 References

1. Alberts, B., *et al.* (1995). Molecular Biology of the Cell (3rd ed.). *Trends in Biochemical Sciences*.
2. Miller, P.W., *et al.* (2013). The evolutionary origin of epithelial cell-cell adhesion mechanisms. *Curr Top Membr* 72, 267-311.
3. Lodish, H., *et al.* (1995). Molecular cell biology (Vol. 3). New York: *Scientific American Books*.
4. O'Donnell, M. J., (2003). Inorganic and organic anion transport by insect renal epithelia. *Biochim Biophys Acta.* 1618, 194-206.
5. Hamilton, K. *et al.*, ed. (2015). Ion Channels and Transporters of Epithelia in Health and Disease. New York, NY: *Springer Berlin Heidelberg*.
6. Harvey, B. J., *et al.* (1988) Intracellular pH controls cell membranes Na^+ and K^+ conductances and transport in frog skin epithelium. *J Gen Physiol* 92, 767-791.
7. Gunter-Smith, P J. *et al.* (1982). Sodium-coupled amino acid and sugar transport by Necturus small intestine. *The Journal of membrane biology* 66.1, 25-39.
8. Robertson, M A., *et al.* (1994). Na^+ transport pathways in secretory acinar cells: membrane cross talk mediated by [Cl^-]. *American Journal of Physiology-Cell Physiology* 267.1, C146-C156.
9. Fowler, M R. *et al.* (2004). Regulation and identity of intracellular calcium stores involved in membrane cross talk in the early distal tubule of the frog kidney. *American Journal of Physiology-Renal Physiology* 286.6, F1219-F1225.

10. Ishibashi, H., *et al.* (1999). Na^+-H^+ exchange in salivary secretory cells is controlled by an intracellular Na^+ receptor. *Proceedings of the National Academy of Sciences* 96.17, 9949-9953.

11. Dinudom, A., *et al.* (1998). Nedd4 mediates control of an epithelial Na^+ channel in salivary duct cells by cytosolic Na^+. *Proceedings of the National Academy of Sciences* 95.12, 7169-7173.

12. Komwatana, P., *et al.* (1996). Cytosolic Na^+ controls and epithelial Na^+ channel via the Go guanine nucleotide-binding regulatory protein. *Proceedings of the National Academy of Sciences* 93.15, 8107-8111.

13. Reddy, M. M., *et al.* (2006). Cytosolic potassium controls CFTR deactivation in human sweat duct. *American Journal of Physiology-Cell Physiology* 291.1, C122-C129.

14. Reddy, M. M., *et al.* (2008). Effect of cytosolic pH on epithelial Na^+ channel in normal and cystic fibrosis sweat ducts. *Journal of Membrane Biology* 225.1-3, 1-11.

15. Wang, Y. B., *et al.* (2014). Sodium transport is modulated by p38 kinase–dependent cross-talk between ENaC and Na, K-ATPase in collecting duct principal cells. *Journal of the American Society of Nephrology* 25.2, 250-259.

16. Elborn, J. S., *et al.* (2016). The effect of CFTR modulation on the disease progression of cystic fibrosis in the era of precision medicine. *Journal of Cystic Fibrosis* 15.2. e20.

17. Haq, I. J., *et al.* (2016). Airway surface liquid homeostasis in cystic fibrosis: pathophysiology and therapeutic targets. *Thorax* 71.3, 284-287.

18. Hanukoglu, I., (2016). Epithelial sodium channel (ENaC) family: Phylogeny, structure–function, tissue distribution, and associated inherited diseases. *Gene* 579.2, 95-132.

19. Staub, O., *et al.* (1997). Regulation of stability and function of the epithelial Na^+ channel (ENaC) by ubiquitination. *The EMBO journal* 16.21, 6325-6336.

20. Chapman, A. D. (2009). Numbers of living species in Australia and the world. *Australian biodiversity information services*, 1-78.

21. Brown, V. K., (1982). The phytophagous insect community and its impact on early succesional habitats. *Proceedings of the 5. International Symposium on Insect-Plant Relationships. Wageningen,* 1-4.

22. Bergstrom, D. M., (2005). Biological invasions in the Antarctic: extent, impacts and implications. *Biol Rev* 80, 4572.

23. Phillips, J., (1981). Comparative physiology of insect renal function. *American Journal of Physiology-Regulatory, Integrative and Comparative Physiology* 241.5, R241-R257.

24. Edney, E. B., (2012). Water balance in land arthropods. Vol. 9. *Springer Science & Business Media*.

25. Ramsay, J. A., (1964). The rectal complex of the mealworm Tenebrio molitor, L.(*Coleoptera, Tenebrionidae*). *Philosophical Transactions of the Royal Society of London B: Biological Sciences* 248.748, 279-314.

26. Nation, L. J., (2002). Insect physiology and biochemistry. *CRC Press INC* 1, 485.

27. Maddrell, S.H. P., (1981). The functional design of the insect excretory system. *J. exp. Biol.* 90, 1-15.

28. O'Donnell, M. J., *et al.* (1983). Paracellular and transcellular routes for water and solute movements across insect epithelia. *Journal of Experimental Biology* 106.1, 231-253.

29. Maddrell, S. H. (1964). Excretion in the Blood-Sucking Bug, *Rhodnius Prolixus* Stal. Ii. the Normal Course of Diuresis and the Effect of Temperature. *The Journal of experimental biology* 41, 163–176.

30. Gioino, P., *et al.* (2014). Serotonin triggers cAMP and PKA-mediated intracellular calcium waves in Malpighian tubules of *Rhodnius prolixus*. *American Journal of Physiology-Regulatory, Integrative and Comparative Physiology* 307.7, R828-R836.

31. Lima, M. M., *et al.* (2012). Investigation of Chagas disease in four periurban areas in northeastern Brazil: epidemiologic survey in man, vectors, non-human hosts and reservoirs. *Transactions of the Royal Society of Tropical Medicine and Hygiene* 106.3, 143-149.

32. Beaty, B. J. *et al.* (2005). The Biology of Disease Vectors. *Elsevier Academic Press* 785.

33. Sargsyan, V. *et al.* (2011). Phosphorylation via PKC regulates the function of the Drosophila odorant co-receptor. *Frontiers in cellular neuroscience* 5, 5.

34. Chapman R. F. (2012). The Insects: Structure and Function. *Cambridge University Press* 954.

35. Buxton, P. A. (1930). The biology of a blood-sucking bug, *Rhodnius prolixus*. *Transactions of the Royal Entomological Society of London* 78.2, 227-256.

36. Coast, G. M., *et al.* (2010). Neurohormones implicated in the control of Malpighian tubule secretion in plant sucking heteropterans: The stink bugs *Acrosternum hilare* and *Nezara viridula*. *Peptides* 31.3, 468-473.

37. Ianowski, J. P., *et al.* (2004). Na^+ competes with K^+ in bumetanide-sensitive transport by Malpighian tubules of *Rhodnius prolixus*. *Journal of Experimental Biology* 207.21, 3707-3716.

38. Ianowski, J. P., *et al.* (2010). The antidiuretic neurohormone RhoprCAPA-2 downregulates fluid transport across the anterior midgut in the blood-feeding insect *Rhodnius prolixus*. *American Journal of Physiology-Regulatory, Integrative and Comparative Physiology* 298.3, R548-R557.

39. Wigglesworth, V. B., *et al.* (1962). Histology of the Malpighian tubules in *Rhodnius prolixus* Stål (Hemiptera). *Journal of Insect Physiology* 8.3, 299-307.

40. Haley, C. A., *et al.* (1997). KCl reabsorption by the lower malpighian tubule of *Rhodnius prolixus*: inhibition by Cl^- channel blockers and acetazolamide. *Journal of insect physiology* 43.7, 657-665.

41. Mori, T., *et al.* (2013). Chemical library screening for WNK signalling inhibitors using fluorescence correlation spectroscopy. *Biochem. J.* 455, 339-345.

42. Ianowski, J. P., *et al.* (2001). Transepithelial potential in Malpighian tubules of *Rhodnius prolixus*: lumen-negative voltages and the triphasic response to serotonin." *Journal of Insect Physiology* 47.4, 411-421.

43. Ianowski, J. P., *et al.* (2002). Intracellular ion activities in Malpighian tubule cells of *Rhodnius prolixus*: evaluation of Na^+-K^+-$2Cl^-$ cotransport across the basolateral membrane.*Journal of Experimental Biology* 205.11, 1645-1655.

44. Beyenbach, K. W., *et al.* (2009). Signaling to the apical membrane and to the paracellular pathway: changes in the cytosolic proteome of *Aedes* Malpighian tubules. *Journal of Experimental Biology* 212.3, 329-340.

45. Piala, A. T., *et al.* (2014). Chloride sensing by WNK1 kinase involves inhibition of autophosphorylation. *Science signaling* 7.324, ra41.

46. Alessi, D. R., *et al.* (2014). The WNK-SPAK/OSR1 pathway: master regulator of cation-chloride cotransporters. *Sci. Signal.* 7.334, re3-re3.

47. Ashby, M. C., *et al.* (2002). Polarized calcium and calmodulin signaling in secretory epithelia. *Physiol Rev* 82, 701-734.

48. Jaffe, L. F. (2010). Fast calcium waves. *Cell Calcium* 48, 102-113.

49. Nagata, J., *et al.* (2007). Lipid rafts establish calcium waves in hepatocytes. *Gastroenterology* 133, 256-267.

50. Ross, W. N. (2015). Understanding calcium waves and sparks in central neurons. *Nat Rev Neurosci* 13, 157-168.

51. Peterson, O. H., *et al.* (2008). Polarized calcium signaling in exocrine gland cells. *Annu Rev. Physiol.* 70, 273-299.

52. Jaffe, L. F. (2008). Calcium waves. *Phil. Trans. R. Soc.B* 363, 1311-1316.

53. Clapham, D. E. (1995). Calcium Signaling. *Cell* 80, 259-268.

54. Smedler, E., *et al.* (2014). Frequency decoding of calcium oscillations. *Biochimica et Biophysica Acta* 1840, 964-969.

55. Mercier-Zuber, A., *et al.* (2011). Role of SPAK and OSR1 signalling in the regulation of NaCl cotransporters. *Current opinion in nephrology and hypertension* 20.5, 534-540.

56. Yamaguchi, M. (2005). Role of regucalcin in maintaining cell homeostasis and function. *International journal of molecular medicine* 15.3, 371-390.

57. Thastrup, J. O., *et al.* (2012). SPAK/OSR1 regulate NKCC1 and WNK activity: analysis of WNK isoform interactions and activation by T-loop trans-autophosphorylation. *Biochemical Journal* 441.1, 325-337.

58. Kahle, K. T., *et al.* (2010). Phosphoregulation of the Na^+–K^+–$2Cl^-$ and K^+–Cl^- cotransporters by the WNK kinases. *Biochimica et Biophysica Acta (BBA)-Molecular Basis of Disease*1802.12, 1150-1158.

59. Wu, Y., *et al.* (2014). Hypotonicity stimulates potassium flux through the WNK-SPAK/OSR1 kinase cascade and the Ncc69 sodium-potassium-2-chloride cotransporter in the *Drosophila* renal tubule. *Journal of Biological Chemistry* 289.38, 26131-26142.

60. Ponce-Coria, J., *et al.* (2012). Calcium-binding protein 39 facilitates molecular interaction between Ste20p proline alanine-rich kinase and oxidative stress response 1 monomers. *American Journal of Physiology-Cell Physiology* 303.11, C1198-C1205.

61. Mercier-Zuber, A., *et al.* (2011). Role of SPAK and OSR1 signalling in the regulation of NaCl cotransporters. *Current opinion in nephrology and hypertension* 20.5, 534-540.

62. Ponce-Coria, J., *et al.* (2014). A novel Ste20-related proline/alanine-rich kinase (SPAK)-independent pathway involving calcium-binding protein 39 (Cab39) and serine threonine kinase with no lysine member 4 (WNK4) in the activation of Na-K-Cl cotransporters. *Journal of Biological Chemistry* 289.25, 17680-17688.

63. Hofer, A. M., *et al.* (1994). Direct measurement of free Ca^{2+} in organelles of gastric epithelial cells. *American Journal of Physiology-Gastrointestinal and Liver Physiology* 267.3, G442-G451.

6.0 Appendix I

6.1 Source of Ca^{2+}

To investigate how the change in ion transport modulates intracellular Ca^{2+} oscillations we investigated the source of intracellular Ca^{2+}. Gioino *et al.* showed that Ca^{2+} free ringer solution with EGTA had no effect on Ca^{2+} oscillations. EGTA is strong chelator of Ca^{2+} that cannot cross the cell membrane. Thus, there is no Ca^{2+} available outside the cell for uptake. This suggests, that Ca^{2+} oscillations are not driven from extracellular Ca^{2+} and the Ca^{2+} oscillations observed are driven from intracellular Ca^{2+} stores. The two intracellular Ca^{2+} stores that may be driving the oscillations are the endoplasmic reticulum (ER) and the mitochondria.

Thapsigargin is a chemical agent that blocks sarco/endoplasmic reticulum Ca^{2+}-ATPase (SERCA) pump in the endoplasmic reticulum, which is responsible for re-uptake of Ca^{2+} from the cytosol. Thus, if we block SERCA using thapsigargin, theoretically it should cease Ca^{2+} oscillations. However, Figure 18 shows that there is a sudden increase of Ca^{2+}, followed by regeneration of oscillations. This means that the oscillations are not driven by the ER.

Ruthenium red is a chemical agent that blocks mitochondria uniporter, disrupting its membrane potential. Figure 19 shows that addition of ruthenium red, ceases Ca^{2+} oscillations. This highlights mitochondria as a probable source that drives intracellular Ca^{2+} oscillations.

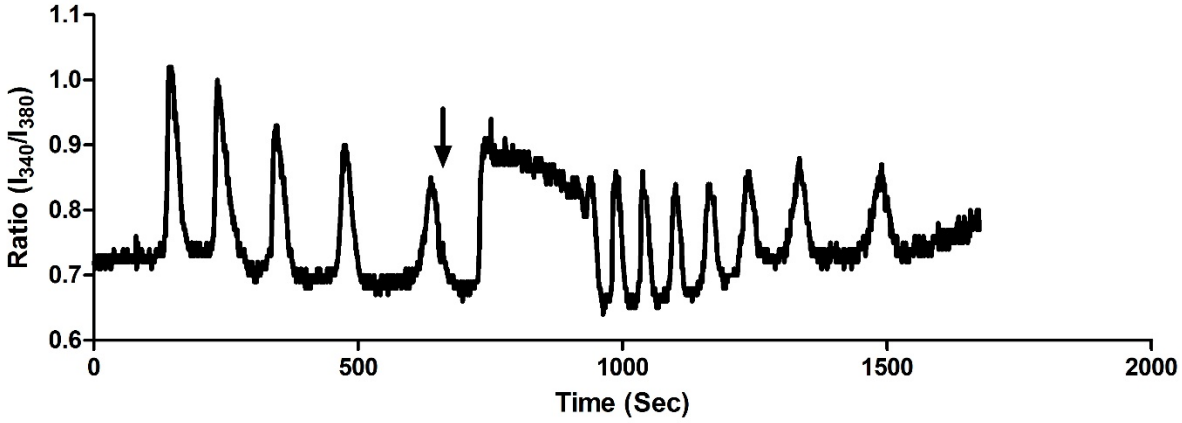

Figure 19: A sample trace of the effect of thapsigargin (1 µmol l^{-1}) on Ca^{2+} oscillations. The Malpighian tubules were incubated with Fura2-AM, probenecid and control saline for 60 min. After incubation, Fura2-AM was washed out with saline solution containing probenecid (1 mmol l^{-1}). The tubules were stimulated with (1µmol l^{-1}) Serotonin. The arrow marks the time at which thapsigargin was added to the saline solution bath.

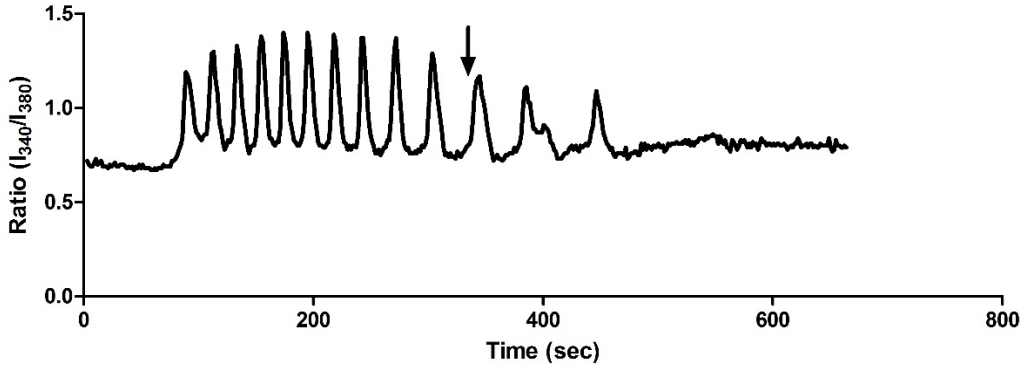

Figure 20: A sample trace of the effect of ruthenium red (1 µmol l^{-1}) on Ca^{2+} oscillations. The Malpighian tubules were incubated with Fura2-AM, probenecid and control saline for 60 min. After incubation, Fura2-AM was washed out with saline solution containing probenecid (1 mmol l^{-1}). The tubules were stimulated with (1µmol l^{-1}) Serotonin. The arrow marks the time at which ruthenium red was added to the saline solution bath.

6.2 MS identified proteins

Table 2: Proteins of interest found in the cytosol fraction, identified against *D. melanogaster* database, and their comparison between control and serotonin stimulated samples. Proteins in bold indicate a post translational phosphorylated protein.

NCBI GI Accession #	Protein Name[1]	NCBI GI Accession #	Protein Name[1]	NCBI GI Accession #	Protein Name[1]
85018	Hypothetical protein 2	442623528	Activated Cdc42 kinase-like, isoform E	455392	Tyrosine kinase
481529	**Hypothetical protein**	11176	Phosphoglycerate kinase	514919	Phosphofructokinase
1419489	Tosca	157212	Cgmp-dependent protein kinase	706902	Glucosephosphate isomerase
1698634	**Decapentaplegic protein**	641918	Vacuolar atpase subunit A	974553	Carboxypeptidase precursor
2624054	Protein tyrosine kinase	2133673	Hypothetical protein 1	1854505	1-phosphatidylinositol 3-kinase
6014919	Recname: Full=DEAD-box helicase Dbp80 [Drosophila melanogaster]	**2760522**	**Toucan protein**	2832418	Capsuleen
		3047011	**Ser/Thr kinase**	2852361	Calcium binding EF-hand protein precursor
10765559	Hexokinase-C	**5281068**	**RECQ helicase homolog**	**6014919**	**Recname: Full=DEAD-box helicase Dbp80 [Drosophila melanogaster]**
17136612	Vacuolar H[+] atpase 16kd subunit 1, isoform A	6063416	Calreticulin		
17136988	Wee1 kinase	17136402	Protein C kinase 53E, isoform A	6573196	Na/K-atpase alpha subunit isoform 2
17137372	**Neurospecific receptor kinase**	17136708	Downstream of receptor kinase, isoform A	**6739532**	**LPS-responsive kinase**
17737302	Adenine nucleotide translocase 2, isoform A	17136796	Vacuolar H[+]-atpase 55kd subunit, isoform B	6760466	Integrin-linked kinase
17864380	**MAP kinase activated protein-kinase-2, isoform B**	17136892	Vacuolar H[+] atpase 14kd subunit 1	17137450	Regulatory particle non-atpase 3, isoform A
21355577	Galactokinase, isoform B	17136902	Camp-dependent protein kinase 1, isoform D	17137684	Vacuolar H[+] atpase 13kd subunit, isoform A
21358171	Vacuolar H[+] atpase 100kd subunit 1, isoform E	17137738	Regulatory particle triple-A atpase 1	17647573	Lethal with a checkpoint kinase, isoform A
21489908	MICAL long isoform	17737775	Vacuolar H[+]-atpase 26kd subunit, isoform B	17647809	Phosphofructokinase, isoform A
24585051	Sterol carrier protein X-related thiolase	17738151	Regulatory particle triple-A atpase 5	17647857	Replication factor C subunit 4
24642465	Calpain C	17981717	Catalase	**17864464**	**Cannonball**
24642539	Calnexin 14D	18079297	Hexokinase A, isoform A	19920728	Regulatory particle non-atpase 11

24648409	Dicarboxylate carrier 2, isoform A
24651125	ATP synthase-gamma chain, isoform A
24652897	**Ornithine decarboxylase antizyme, isoform C**
24655003	**Dodeca-satellite-binding protein 1, isoform G**
24762445	Calcium atpase at 60A, isoform B
161076448	Protein kinase related to protein kinase N, isoform G
221330000	Laccase 2, isoform E
221330448	**Focal adhesion kinase, isoform D**
429892356	**Scavenger receptor class C type II, partial**
442614522	ATP synthase-beta, isoform C
442623526	Activated Cdc42 kinase-like, isoform D
665410673	WNK

18543319	Vacuolar H[+] atpase AC39 subunit 1
18860095	Mrna-capping-enzyme
19920408	Regulatory particle triple-A atpase 6
21355083	Cathd
21355551	Vacuolar H[+] atpase 36kd subunit 1
21357061	Vacuolar H[+] atpase 100kd subunit 4
22026816	Adenylate kinase-2
24581952	Helicase at 25E, isoform A
24583984	Vacuolar H[+] atpase 68 kda subunit 2, isoform A
24584673	Vacuolar H[+]-atpase SFD subunit, isoform B
24586303	Boca
24649446	Regulatory particle triple-A atpase 2, isoform A
24651092	CAP-D2 condensin subunit
24654282	Protein C kinase 53E, isoform B
24658274	Cyclin-dependent kinase 9
24762614	Sterile20-like kinase, isoform B
45553053	Mucin 68Ca
56311435	Calcineurin A at 14F, isoform A
116008198	No circadian temperature entrainment, isoform A
226303480	Cgmp-dependent protein kinase
281359545	Plasma membrane calcium atpase, isoform N
281361934	Cadherin 89D
386765437	Molecule interacting with casl, isoform L

19922628	Carbonyl reductase, isoform B
20128937	Vacuolar H[+] atpase 36kd subunit 3, isoform B
21357745	Glutamine:fructose-6-phosphate aminotransferase 2
24581010	Glycogen phosphorylase, isoform A
24581352	**Toucan, isoform B**
24583992	Vacuolar H[+] atpase 68kd subunit 1, isoform A
24586044	Tyrosine decarboxylase 2
24639306	Monocarboxylate transporter 1, isoform A
24642547	Protein phosphatase 2B at 14D, isoform A
24646066	**Bloom syndrome helicase ortholog**
24649111	Cardinal
24651451	Regulatory particle triple-A atpase 6-related
24655085	Phosphoenolpyruvate carboxykinase
24663043	Pericardin
24665368	**Multiple inositol polyphosphate phosphatase 1, isoform A**
28571841	PTEN-like phosphatase, isoform B
28573187	Phosphoribosylamidotransferase, isoform A
28573326	Phosphofructokinase, isoform C
28574621	**Neurocalcin, isoform A**
45553117	**Regulatory particle non-atpase 12-related**
59936685	Cadherin 99C
85725280	Protein kinase C delta, isoform C

	442615406	Sarcoplasmic calcium-binding protein, isoform C	111145037	Glyceraldehyde 3 phosphate dehydrogenase 2, partial
	442624604	Alpha-catenin related, isoform C	221330084	Calmodulin-binding transcription activator, isoform F
	442624643	Regulatory particle non-atpase 8, isoform B	281361487	Regulatory particle triple-A atpase 3-related, isoform C
	665402139	Calpain-A, isoform D	1303450	Frayed
	17647815	Camp-dependent protein kinase R2, isoform A	386765439	Molecule interacting with casl, isoform M
	442614533	Calcium/calmodulin-dependent protein kinase II, isoform K	**386769428**	**SCAR, isoform C**
	281359589	Calcium/calmodulin-dependent protein kinase II, isoform J	442616155	Phosphodiesterase 9, isoform D
			442616948	Carnation, isoform C
			442620344	Camguk

[1]List of proteins based on SpectrumMill scoring index. The list of proteins focuses on kinases, phosphatases, calcium binding proteins and other proteins that may be involved in ion transport.

Table 3: Proteins of interest found in the membrane fraction, identified against *D. melanogaster* database, and their comparison between control and serotonin stimulated samples. Proteins in bold indicate a post translational phosphorylated protein.

NCBI GI Accession #	Identified Protein [1]	NCBI GI Accession #	Identified Protein[1]	NCBI GI Accession #	Identified Protein[1]
17737302	Adenine nucleotide translocase 2, isoform A	8070	H3 histone	11176	Phosphoglycerate kinase
22026816	Adenylate kinase-2	442614522	Actin 57B	442615594	Bent, isoform F
442624604	Alpha-catenin related, isoform C	17530805	Alpha spectrin, isoform B	2133673	**Bloom syndrome helicase ortholog**
857563	Arginine kinase	17136564	Alpha-Tubulin at 84B	**281364702**	**Cadmus, isoform A**
21429768	At20865p	442614522	ATP synthase-beta, isoform C	73620980	Camguk
442623736	Atypical protein kinase C, isoform J	217338	Bellwether	**21357127**	Canoe, isoform I
442614471	Bent, isoform I	24655737	Beta spectrin, isoform B	21489904	CAP, isoform R
18858189	Caf1-180	158739	Beta-1 tubulin	17136902	CAP-D2 condensin subunit
45551541	Calcium-independent phospholipase A2 VIA, isoform B	24658560	Beta-Tubulin at 56D, isoform B	17933512	**Carnation, isoform C**
221330084	**Calmodulin-binding transcription activator, isoform F**	103519	Bicaudal C, isoform A	17865841	Cg32113
24642539	Calnexin 14D	**386765517**	**Cadherin 86C, isoform F**	24661707	Clathrin heavy chain, isoform A
24642465	**Calpain C**	6063416	Calreticulin	17136708	Downstream of receptor kinase, isoform A
665402139	Calpain-A, isoform D	17981717	Catalase	19527633	Dynein heavy chain 64C, isoform I
78706884	CENP-ana, isoform A	19920794	CG9140, isoform A	**17864478**	**Glcat-S, isoform C**
24644205	**Ceramide kinase, isoform A**	17647135	Elongation factor 1alpha100e, isoform A	21357745	Glycerol-3-phosphate dehydrogenase
20384914	CG13367 truncation 1	17864154	Elongation factor 1alpha100e, isoform A	28574007	Hepatocyte growth factor regulated tyrosine kinase substrate, isoform C
442626474	**CG18304, isoform D**	706902	Glucosephosphate isomerase	10765559	Hexokinase-C
116007274	Cg34124	4580727	Glucosephosphate isomerase	24581780	**Hypothetical protein**
442618971	CG34383, isoform I	45553475	Glutamate dehydrogenase, isoform F	**24646066**	**Hypothetical protein 2**
665393752	CG42795, isoform G	11176	Glutamine:fructose-6-phosphate aminotransferase 2	24667933	Integrin linked kinase, isoform A
		22023983	Glyceraldehyde 3 phosphate dehydrogenase 1, isoform A	17137000	Male sterile (3) 72Dt
		442616948	**Glyceraldehyde 3 phosphate dehydrogenase 2, partial**	157594	MICAL short isoform
				19920794	Mip04331p
				20908094	Moesin, isoform M
				442616758	Neural conserved at 73EF, isoform I

21357561	CTP:phosphocholine cytidylyltransferase 2
17137468	**Decapentaplegic, isoform A**
24586270	Dilute class unconventional myosin, isoform C
11096177	DNA polymerase zeta catalytic subunit
17737403	DNA replication-related element factor, isoform A
5734514	**Drosophila dodeca-satellite protein 1**
386769771	**Dynein heavy chain at 36C**
442629130	Enhancer of bithorax, isoform H
157554	G protein-coupled receptor kinase
25009987	Gh07765p
17737967	Heat shock protein cognate 4, isoform A
281361147	HECT and RLD domain containing protein 2 ortholog
10765181	Hexokinase-t2
665393263	Holocarboxylase synthetase, isoform C
6760466	Integrin-linked kinase
17985997	Inverted repeat-binding protein, isoform A
255760070	Ip07924p
7159652	Kettin
24585145	Lethal (2) 37Cc, isoform A
62472261	Mi-2, isoform B
325530376	Mip14694p
20128937	H3 histone
18079297	Hexokinase A, isoform A
78707122	Histone H2A
2133673	Hypothetical protein 1
157294	Inositol 1,4,5-trisphosphate receptor
17137572	Karst, isoform E
23344920	Kinase suppressor of ras
442620118	Leucine-rich repeat kinase, isoform D
24581780	Marcal1
6063416	Mitochondrial acyl carrier protein 1, isoform C
386765437	Molecule interacting with casl, isoform L
320544538	Muscle-specific protein 300 kda, isoform B
442630302	Muscle-specific protein 300 kda, isoform D
4580727	Phosphate transporter precursor
24657148	Protein tyrosine phosphatase-ERK/Enhancer of Ras1
706902	PTEN-like phosphatase, isoform B
24583992	Re74713p
25013056	Rh61958p
17647897	Ribosomal protein s5a, isoform A
17933512	Sarcoglycan delta, isoform A
3047011	**Ser/Thr kinase**
442631934	**Sodium chloride cotransporter 69, isoform E**
116007492	Ste20-like kinase, isoform A
24762614	Sterile20-like kinase, isoform B
3288870	Phosphatidylinositol 4-phosphate 5-kinase
24657148	**Phosphotyrosine phosphatase**
442619798	Protein kinase D, isoform G
161076448	Protein kinase related to protein kinase N, isoform G
433182	**Protein tyrosine phosphatase 10D, isoform F**
54650560	Rabconnectin-3A
3288870	**Receptor protein tyrosine phosphatase**
281363101	Recname: Full=Protein pecanex [Drosophila melanogaster]
442624643	Regulatory particle non-atpase 8, isoform B
24649446	Regulatory particle triple-A atpase 2, isoform A
17864154	Rh04426p
24651092	RNA helicase
25013056	Sec71 ortholog
17136720	**Small conductance calcium-activated potassium channel, isoform S**
283668	**Suppressor of Under-Replication**
1498252	Tyrosine kinase substrate

442615594	Moesin, isoform M	21355551	Stress-sensitive B, isoform C	
45553053	Mucin 68Ca	**20908094**	**TPA_exp: TITIN**	
24665368	**Multiple inositol polyphosphate phosphatase 1, isoform A**	21358171	Vacuolar H[+] atpase 100kd subunit 1, isoform E	
320544544	Muscle-specific protein 300 kda, isoform G	17136612	Vacuolar H[+] atpase 16kd subunit 1, isoform A	
386766168	**Na/Ca-exchange protein, isoform G**	20128937	Vacuolar H[+] atpase 36kd subunit 3, isoform B	
116008198	**No circadian temperature entrainment, isoform A**	21355787	Vacuolar H[+] atpase M8.9 accessory subunit	
455163	**P90 ribosomal S6 kinase**			
1272420	Phosphoinositide 3-kinase			
251174	Protein phosphatase from PCR fragment D5, partial			
18858005	Pyruvate dehydrogenase phosphatase, isoform A			
21064465	Re36839p			
51092065	Re42129p			
442629639	**Sallimus, isoform P**			
442615406	Sarcoplasmic calcium-binding protein, isoform C			

[1]List of proteins based on SpectrumMill scoring index. The list of proteins focuses on kinases, phosphatases, calcium binding proteins and membrane proteins that may be involved in ion transport.